ISA Transactions 95 (2019) 330–345

Contents lists available at ScienceDirect

ISA Transactions

journal homepage: www.elsevier.com/locate/isatrans

Practice article

Fault tolerant control for modified quadrotor via adaptive type-2 fuzzy backstepping subject to actuator faults

Samir Zeghlache [a,*], Ali Djerioui [b], Loutfi Benyettou [b], Tarak Benslimane [b], Hemza Mekki [b], Abderrahmen Bouguerra [b]

[a] LASS, Laboratoire d'Analyse des Signaux et Systèmes, Department of Electrical Engineering, Faculty of Technology, University of M'sila, BP 166 Ichbilia, Msila, Algeria
[b] LGE, Laboratoire de Génie Electrique, Department of Electrical Engineering, Faculty of Technology, University of M'sila, BP 166 Ichbilia, Msila, Algeria

HIGHLIGHTS

- A robust controller based on backstepping and type-2 fuzzy logic are designed.
- Modeling the new modified quadrotor aircraft in healthy and faulty operation.
- Proof of stability using Lyapunov theory are given.
- Comparative study with other techniques proposed in literature.

ARTICLE INFO

Article history:
Received 3 August 2018
Received in revised form 27 April 2019
Accepted 29 April 2019
Available online 14 May 2019

Keywords:
Backstepping control
Type-2 fuzzy logic systems
Adaptive control
Robust control
Modified quadrotor

ABSTRACT

In this paper, a robust attitude and position control of a novel modified quadrotor unmanned aerial vehicles (UAV) which has higher drive capability as well as greater robustness against actuator faults than conventional quad-rotor UAV has been developed. A robust backstepping controller with adaptive interval type-2 fuzzy logic is proposed to control the attitude and position of the modified quadrotor under actuator faults. Besides globally stabilizing the system amid other disturbances, the insensitivity to the model errors and parametric uncertainties are the asset of the backstepping approach. The adaptive interval type-2 fuzzy logic as fault observer can effectively estimate the lumped faults without the knowledge of their bounds for the modified quadrotor UAV. Additionally, the type-2 fuzzy systems are utilized to approximate the local nonlinearities of each subsystem under actuator faults, next and in order to achieve the expected tracking performance, we used Lyapunov theory stability and convergence analysis to online adjust adaptive laws. As a result, the uniformly ultimate stability of the modified quadrotor system is proved. Finally, the performances of the proposed control method are evaluated by simulation and the results demonstrate the effectiveness of the proposed control strategy for the modified quadrotor in vertical flights in presence of actuator faults.

1. Introduction

In the past last years, a growing interest has been shown in robotics. In fact, several industries (automotive, medical, manufacturing, space, ...), require robots to replace men in dangerous, boring or onerous situations. A wide area of the development efforts in this field is dedicated to aerial platform especially multi rotors ones.

The multi-rotors aerial platforms are underactuated systems and the state variables are highly coupled. In order to control multi-rotors UAV, interesting strategies are made to deal with trajectory tracking problems. In [2,3], a PID controller for attitude stabilization of a quadrotor UAV is presented. This research successfully demonstrated through experiments that a simple PID control is sufficient for stable flight. On the other hand, the inconvenient of this method is being convenient only for the linear systems and not for nonlinear ones except when making some hypothesis. Some papers presented the control of the quadrotor in 6 DOF using Lyapunov theory [4–6]. According to this technique, it is possible to ensure, under certain conditions, the asymptotical stability of the helicopter; without guaranteying a good robustness. In [7,8], adaptive control techniques for

* Corresponding author.
E-mail addresses: samir.zeghlache@univ-msila.dz (S. Zeghlache), alidjerioui@yahoo.fr (A. Djerioui), benyettou_letfi@yahoo.fr (L. Benyettou), bens082002@yahoo.fr (T. Benslimane), hemza.mekki@g.enp.edu.dz (H. Mekki), rah_bou@yahoo.fr (A. Bouguerra).

https://doi.org/10.1016/j.isatra.2019.04.034
0019-0578/

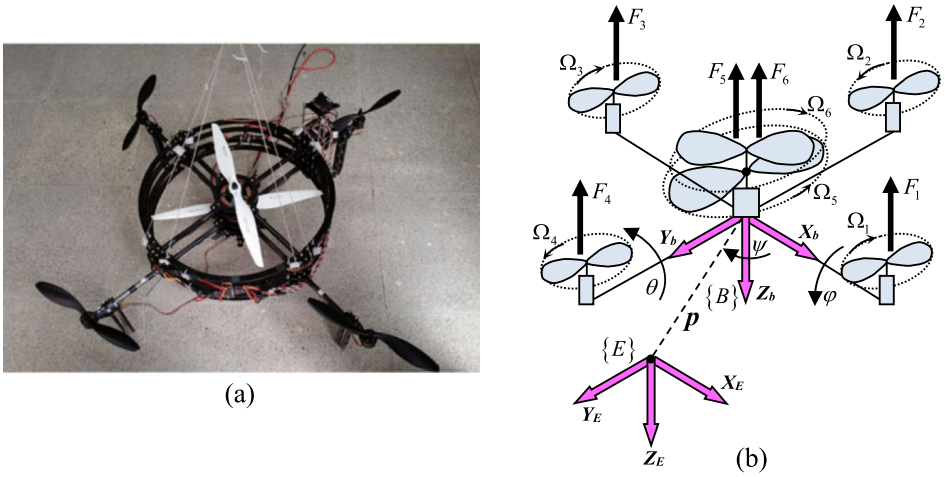

Fig. 1. Modified quadrotor (a) portrait (b) configuration [1].

an autonomous helicopter have been presented. These methods provide good performance with parametric uncertainties and unmodeled dynamics. In [9–11], a trajectory planning controller for UAV helicopter based on Linear Quadratic Regulation (LQR) was designed and validated. H∞ methods are used in UAV helicopter control to synthesize controllers achieving stabilization with guaranteed performance. To use H∞ methods, the control designer expresses the control problem as a mathematical optimization problem to find the controller that solves this problem. H∞ techniques have the advantage over classical control techniques in that they are readily applicable to problems involving multivariate systems with cross-coupling between channels; disadvantages of H∞ techniques include the level of mathematical understanding needed to apply them successfully and the need for a reasonably good model of the system to be controlled. In [12], simulation results in the nearby equilibrium point were considered satisfactory using H∞ methods to control UAV helicopter. A feedback control algorithm proposed in [13,14] to control the quadrotor helicopter succeeded in handling the states coupling problem, but without restraining the uncertainty of model interference. In [15,16], the authors used the backstepping control. In these works, the convergence of the quadrotor internal states is guaranteed, but lot of computation is required. In the literature the sliding mode control technique has been used to control quadrotors. The advantage of this approach is its insensitivity to the model errors and parametric uncertainties, as well as the ability to globally stabilize the system in the presence of other disturbances [17]. In [18], a sliding mode control has been used to stabilize a quadrotor helicopter. A controller based on backstepping and sliding mode techniques for miniature quadrotor helicopter is presented in [19], the major disadvantage of this method is the chattering effect. In [20], a second order sliding mode control is proposed to control the autonomous helicopter showing a good ability to eliminate the chattering and bad insensitivity to noise. In the literature, the most proposed control strategies are addressed to conventional quadrotor UAV. Later, present deficiency in term of driving ability. To increase hardware redundancy and enhance Fault Tolerant Control (FTC) capability, many modified quadrotor structures are proposed by adding generally two or four actuators producing conventional hexarotor and octorotor [21–35]. A novel modified quadrotor configuration has been proposed in [1] with the aim of increasing stability and payload lifting capacity of the conventional quadrotor. It is designed in a way that the dynamics and steering principles are kept as simple as conventional quadrotors. The modified quadrotor has two additional coaxial rotors in the center, rotating in a constant speed and opposite directions (Fig. 1). The motion control is carried out by the four peripheral rotors, like a conventional quadrotor. In other words, speed of these motors varies during flight, whereas the coaxial rotors spin in constant values. The additional coaxial propellers increase rotor area and improve the stability accordingly, even in comparison with conventional hexarotor and octorotor [21–35]. Two coaxial propellers are completely identical and rotate at constant speeds in opposite directions. As a result, the gyroscopic and drag torques of each propeller will be eliminated. These rotors do not therefore impose any extra term in the dynamics of the vehicle. On the other hand, the thrust produced by each of the coaxial propellers is in the same direction, helping the robot to carry heavier payloads. Also, in this modified configuration, a major portion of the payload weight is compensated by coaxial rotors causing the 4 controlling motors rotate at lower speeds. This modified configuration is much better than the conventional quadrotor in which all the payload weight is carried by the four motors forcing the rotors to rotate at much higher speeds [1]. Furthermore, the modified quadrotor can be designed to accommodate the case of motors failure keeping the helicopter flying. In fact, the conventional hexarotor and octorotor fault tolerant control are widely investigated in actuator and sensor fault; which is not the case of the novel structure of modified quadrotor considered in this paper [21–35].

It is noted that all of these previous works make the assumption that the aerial vehicle is fault-free. Therefore, the motivation of our present research is to provide an effective fault reconstruction and tolerance strategy for the modified quadrotor.

Fuzzy logic systems are known as powerful approximations [36]. They have been tested extensively to control uncertain nonlinear systems. The advantage of these approaches is the universal approximation properties. Recently, various adaptive fuzzy control methods have been developed for different classes of uncertain nonlinear systems [37]. In the present work, an adaptive and robust control algorithm based on backstepping technique is proposed for a class of systems encountered mainly in aerial vehicles. Generally the dynamic model of the aerial vehicles is composed by several interconnected subsystems. The type-2 fuzzy systems are utilized to identified the local nonlinearities of each subsystem, and then, the fuzzy parameters are on-line adjusted by adaptive laws with stability and convergence analysis of the Lyapunov theory in order to achieve the expected tracking performance. The interval type-2 fuzzy logic system (IT2FLS) is used to approximate the unknown part of modified quadrotor dynamic equation, avoiding its complex modeling. In

addition, the backstepping approach can deal with internal and external disturbances as well as fault effects.

The control problem considered in this work is to perform asymptotic position and attitude tracking of a modified quadrotor subject to actuator faults by designing a fault tolerant flight controller.

Compared to the existing works in the literature [1,23–28,30,31,34,35,38–49], the contributions of this paper are highlighted in the following aspects:

- In [23–26,28,30,34,38,39], the authors proposed a passive fault tolerant control (PFTC), which requires the fault estimation. This design method becomes very difficult in case of severe faults. In the present paper, a novel adaptive type-2 fuzzy backstepping control (AT2FBC) as FTC is designed to maintain a good trajectory tracking of a modified quadrotor with actuator faults, where the IT2FLS has been used for fault detection and reconstruction.
- In [35] authors propose a complex fault tolerant concept based on adaptive RBFNN (Radial Base Function Neural Network) combined with fuzzy sliding mode strategy for eight rotors helicopter. Where the RBFNN is used to approximate the uncertainties caused by the actuator faults and the fuzzy inference system has been used only to approximate the discontinue part of the sliding mode control. However, the number of hidden neurons selection, center and base widths in RBFNN are determined randomly and require expert's knowledge [50]. To solve RBFNN problem, this paper investigates a simple adaptive type-2 fuzzy systems to approximate the uncertain (due to actuator faults) appearing in the modified quadrotor model and the backstepping strategy to systematically design a non linear controller. In addition, the big in size, the battery life is often far less, and the big cost make the eight rotors helicopter less uses compared to the modified quadrotor.
- Unlike in [1], the adaptive control law, adopted in the present paper, has been implemented in all steps of the backstepping control design, which increases the tolerance of the controller. Moreover, the proposed FTC deals with a defective modified quadrotor, while in [1], a healthy modified quadrotor case is considered.
- An interval type-2 fuzzy neural network is proposed for quadrotor and octorotor aircrafts control [31,40]. This controller's parameters are tuned by an optimal SMC and PD techniques, in order to compensate parametric uncertainties and disturbances. The parameters of this hybrid control are adjusted through an online learning algorithm based on sliding-mode training algorithm and type-2 fuzzy systems adaptive controller. The simulation results, showing a robust reference tracking performance, remain insufficient, because the system global stability validating this control strategy is not discussed. In the present paper, the stability analysis of the closed-loop system is strictly proven.
- Fault detection and reconstruction based on sliding mode observer are given in [41,42]. In the present paper, an adaptive type-2 fuzzy inference system is used to detect and reconstruct the faults.
- In [27,43], a passive FTC applied to the hexarotor and quadrotor helicopters based on backstepping control approach has been proposed. In the present paper, the proposed FTC approach is based on the combination between backstepping control and adaptive interval type-2 fuzzy inference systems. Later, can deal with several classes of faults.
- An intelligent fuzzy control has been tested extensively to control quadrotors in several works such as [44,45]. However, the trial and error problem lead to great limitation of these approaches [46]. In [47], a fuzzy PID controller is designed to control the quadrotor helicopter, to achieve trajectory tracking and to reduce the influence of external disturbances; but it cannot deal with fault effects. In the present paper, an adaptive nonlinear control is proposed to achieve position and angle finite time convergence in uncertainty and actuator faults presence.
- Adaptive control is a control method in which the controller must adapt to the controlled system where parameters vary or are initially uncertain. An adaptive controller for the octorotor and quadrotor helicopters is designed in [26,48,49]. This approach showed a quick and insensitive to external disturbances response, where no precise model is needed. Although, system faults are not taken into account. In the present paper, an adaptive backstepping control based on type-2 fuzzy inference system is proposed as FTC in the presence of model uncertainties, external disturbance and actuator faults.

Inspired by the works cited above, this paper proposes an AT2FBC for modified quadrotor with defective actuators, in order to compensate the fault effect after estimating the uncertainties. Moreover, this paper presents the modeling of the actuator faults which is carried out for the first time on this kind of modified quadrotor. This new fault modeling can be used to develop more innovative control techniques of this kind of modified quadrotor in the future. The proposed FTC is tested in healthy and faulty conditions with other control methods applied recently on modified quadrotor [1]. Performances of these controllers are investigated and compared in terms of trajectory tracking quality. The main contribution of this paper can be summarized as follows:

(1) The dynamic model of modified quadrotor system with uncertain nonlinear coupling is presented firstly. Then, based on the system actuator faults presentation, the mathematical model of modified quadrotor system with actuator faults is given;
(2) A new modified quadrotor helicopter robust control methodology is introduced based on hybrid control of backstepping control and adaptive type-2 fuzzy inference system;
(3) In order to compensate the disturbances and fault effects, an adaptive tuning of controller parameters is proposed. The simulation results demonstrate that the designed FTC is able to maintain satisfactory performance of the modified quadrotor even in the presence actuator faults.
(4) A new adaptive type-2 fuzzy backstepping controller (AT2FBC) is developed to stabilize the modified quadrotor helicopter in its complete nonlinear configuration. Where, decoupling procedure does not need in this approach.

This paper is arranged as follow; in Section 2, nonlinear dynamic model of the modified quadrotor aircraft is introduced in healthy and faulty operation modes. A brief description of IT2FLS is then introduced in Section 3. The modified quadrotor flight controller design based on FTC is presented in Section 4 and simulation results are given and discussed in Section 5. Finally conclusions on the present paper are driven.

Notation:
UAV: Unmanned Aerial Vehicles.
IT2FLS: Interval Type-2 Fuzzy Logic System.
FTC: Fault Tolerant Control.
PFTC: Passive Fault Tolerant Control.

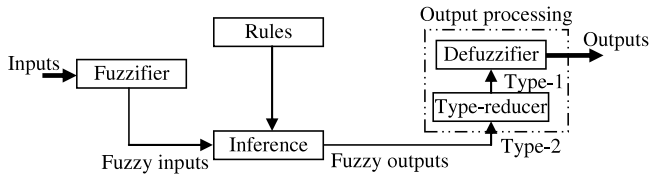

Fig. 2. Type-2 fuzzy logic system structure.

AT2FBC: Adaptive Type-2 Fuzzy Backstepping Control.
SMC: Sliding Mode Control.
LQR: Linear Quadratic Regulation.

2. Dynamical model

2.1. Dynamical modeling of the modified quadrotor in healthy operating mode

The configuration of the modified quadrotor is represented in Fig. 1. It is designed in a way that the dynamics and steering principles are kept as simple as conventional quadrotors. The modified quadrotor has two additional coaxial rotors in the center, rotating in a constant speed and opposite directions (Fig. 1). The motion control is carried out by the 4 peripheral rotors, like a conventional quadrotor. In other words, speed of these motors varies during flight, whereas the coaxial rotors spin in constant values [1].

Let $E(O, X_E, Y_E, Z_E)$ denote an inertial frame, and $B(O', X_b, Y_b, Z_b)$ denote a frame rigidly attached to the modified quadrotor as shown in Fig. 1. The equations governing the motion of the system are obtained using the Euler–Lagrange approach and give the commonly used model [1].

$$\begin{cases} \ddot{x} = \dfrac{1}{m}\{U_1(\sin\theta) - k_1\dot{x}\} \\ \ddot{y} = -\dfrac{1}{m}\{U_1(\sin\varphi\ \cos\theta) + k_2\dot{y}\} \\ \ddot{z} = \dfrac{1}{m}\{-U_1(\cos\varphi\cos\theta) + mg - k_3\dot{z}\} \\ \ddot{\varphi} = \dfrac{1}{I_x}\left\{\dot{\theta}\dot{\psi}\left(I_y - I_z\right) - k_4\dot{\varphi} - J_H\overline{\Omega}\dot{\theta} + U_2\right\} \\ \ddot{\theta} = \dfrac{1}{I_y}\left\{\dot{\varphi}\dot{\psi}\left(I_z - I_x\right) - k_5\dot{\theta} + J_H\overline{\Omega}\dot{\varphi} + U_3\right\} \\ \ddot{\psi} = \dfrac{1}{I_z}\left\{\dot{\varphi}\dot{\theta}\left(I_x - I_y\right) - k_6\dot{\psi} + U_4\right\} \end{cases} \tag{1}$$

where m denotes the total mass. g represents the acceleration of gravity. $k_1, \ldots, k_6$ denote the drag coefficients and positive constants.

$$\overline{\Omega} = \Omega_1 - \Omega_2 + \Omega_3 - \Omega_4 + \Omega_5 - \Omega_6 \tag{2}$$

Ω_i; stand for the angular speed of the propeller i with $i = 1, \ldots, 6$.

I_x, I_y, I_z represent the inertias of the modified quadrotor; J_H denotes the inertia of the propeller; U_1 denotes the total thrust on the body in the z-axis; U_2 and U_3 represent the roll and pitch inputs, respectively; U_4 denotes a yawing moment. $F_j = K_{tj}\Omega_j^2$ with $j = 1, \ldots, 4$ denote the thrust generated by each propeller, $F_r' = K_{tr}'\Omega_r^2$ with $r = 5, 6$ denote the thrust generated by the coaxial propeller, $T_j = -K_{dj}\Omega_j^2$ denote the reaction torque caused by the drag generated by each propeller, $T_r' = -K_{dr}'\Omega_r^2$ denote the reaction torque caused by the drag generated by the coaxial propeller, $\left(K_{tj},\ K_{tr}'\right) > 0$ denotes thrust coefficients, $\left(K_{dj},\ K_{dr}'\right) > 0$ denotes reaction torque coefficients and l denotes the distance from the center of each rotor to the center of gravity.

Assumption 1. The roll, the pitch and the yaw angles (φ, θ, ψ) are bounded as follows: roll angle by $\frac{-\pi}{2} < \varphi < \frac{\pi}{2}$; pitch angle, $\frac{-\pi}{2} < \theta < \frac{\pi}{2}$; and yaw angle, $-\pi < \psi < \pi$.

2.2. Dynamical modeling of the modified quadrotor in faulty operating mode

In healthy operating mode, the motors and the blades mounted on them are supposed similar $\left(K_{tj} = K_t,\ K_{tr}' = K_t',\ K_{dj} = K_d,\ K_{dr}' = K_d', j = 1, \ldots, 4, r = 5, 6\right)$. The relation between the modified quadrotor control inputs and its motors speeds, in this case, is expressed in Eq. (3) [51].

$$U = \begin{bmatrix} U_1 \\ U_2 \\ U_3 \\ U_4 \end{bmatrix} = \begin{bmatrix} K_t & K_t & K_t & K_t & K_t' & K_t' \\ lK_t & 0 & -lK_t & 0 & 0 & 0 \\ 0 & -lK_t & 0 & lK_t & 0 & 0 \\ -K_d & K_d & -K_d & K_d & K_d' & -K_d' \end{bmatrix} \begin{bmatrix} \Omega_1^2 \\ \Omega_2^2 \\ \Omega_3^2 \\ \Omega_4^2 \\ \Omega_5^2 \\ \Omega_6^2 \end{bmatrix} = \Gamma\Omega \tag{3}$$

If a fault occurs in the blades mounted on one of the motors, its thrust and reaction torque coefficients change and the expression $\left(K_{tj} = K_t,\ K_{tr}' = K_t', K_{dj} = K_d,\ K_{dr}' = K_d', j = 1, \ldots, 4, r = 5, 6\right)$ will no longer be correct. The control-speed relation will be updated by introducing a faulty matrix in Eq. (3) as follows [52]:

$$U = \left[\Gamma - \Gamma_f\right]\Omega \tag{4}$$

where Γ_f is the faulty matrix defined as:

$$\Gamma_f = \begin{bmatrix} \beta_1 K_t & \beta_2 K_t & \beta_3 K_t & \beta_4 K_t & \beta_5 K_t' & \beta_6 K_t' \\ \beta_1 lK_t & 0 & -\beta_3 lK_t & 0 & 0 & 0 \\ 0 & -\beta_2 lK_t & 0 & \beta_4 lK_t & 0 & 0 \\ -\beta_1 K_d & \beta_2 K_d & -\beta_3 K_d & \beta_4 K_d & \beta_5 K_d' & -\beta_6 K_d' \end{bmatrix}$$

where $\beta_i (i = 1 \ldots 6)$ is the fault coefficient of each motor. $\beta_i = 0$ refers to healthy actuator, $0 \le \beta_i \le 1$ represents faulty actuator case, and $\beta_i = 1$ reflect a completely damaged actuator condition.

Finally, Eq. (4) can be rearranged as Eq. (5) given in Box I: If we replace Eq. (5) in (1), we obtain:

$$\begin{cases} \ddot{x} = \dfrac{1}{m}\{U_1(\sin\theta) - k_1\dot{x}\} + d_x \\ \ddot{y} = -\dfrac{1}{m}\{U_1(\sin\varphi\ \cos\theta) + k_2\dot{y}\} + d_y \\ \ddot{z} = \dfrac{1}{m}\{-U_1(\cos\varphi\cos\theta) + mg - k_3\dot{z}\} + d_z \\ \ddot{\varphi} = \dfrac{1}{I_x}\left\{\dot{\theta}\dot{\psi}\left(I_y - I_z\right) - k_4\dot{\varphi} - J_H\overline{\Omega}\dot{\theta} + U_2\right\} + d_\varphi \\ \ddot{\theta} = \dfrac{1}{I_y}\left\{\dot{\varphi}\dot{\psi}\left(I_z - I_x\right) - k_5\dot{\theta} + J_H\overline{\Omega}\dot{\varphi} + U_3\right\} + d_\theta \\ \ddot{\psi} = \dfrac{1}{I_z}\left\{\dot{\varphi}\dot{\theta}\left(I_x - I_y\right) - k_6\dot{\psi} + U_4\right\} + d_\psi \end{cases} \tag{6}$$

$$\begin{bmatrix} U_1 \\ U_2 \\ U_3 \\ U_4 \end{bmatrix} = \begin{bmatrix} K_t(1-\beta_1) & K_t(1-\beta_2) & K_t(1-\beta_3) & K_t(1-\beta_4) & K_t'(1-\beta_5) & K_t'(1-\beta_6) \\ lK_t(1-\beta_1) & 0 & -lK_t(1-\beta_3) & 0 & 0 & 0 \\ 0 & -lK_t(1-\beta_2) & 0 & lK_t(1-\beta_4) & 0 & 0 \\ -K_d(1-\beta_1) & K_d(1-\beta_2) & -K_d(1-\beta_3) & K_d(1-\beta_4) & K_d'(1-\beta_5) & -K_d'(1-\beta_6) \end{bmatrix} \begin{bmatrix} \Omega_1^2 \\ \Omega_2^2 \\ \Omega_3^2 \\ \Omega_4^2 \\ \Omega_5^2 \\ \Omega_6^2 \end{bmatrix} \quad (5)$$

Box I.

where the unknown resultant related to the actuator faults are given by:

$$\begin{cases} d_x = -\dfrac{\sin\theta}{m}\left(\beta_1 K_t + \beta_2 K_t + \beta_3 K_t + \beta_4 K_t + \beta_5 K_t' + \beta_6 K_{t8}'\right) \\ d_y = \dfrac{\sin\varphi\cos\theta}{m}\left(\beta_1 K_t + \beta_2 K_t + \beta_3 K_t + \beta_4 K_t + \beta_5 K_t' + \beta_6 K_t'\right) \\ d_z = \dfrac{\cos\varphi\cos\theta}{m}\left(\beta_1 K_t + \beta_2 K_t + \beta_3 K_t + \beta_4 K_t + \beta_5 K_t' + \beta_6 K_t'\right) \\ d_\varphi = -\dfrac{l}{I_x}\left(\beta_1 K_t - \beta_3 K_t\right) \\ d_\theta = -\dfrac{l}{I_y}\left(\beta_4 K_t - \beta_2 K_t\right) \\ d_\psi = -\dfrac{1}{I_z}\left(\beta_2 K_d + \beta_4 K_d + \beta_5 K_d' - \beta_1 K_d - \beta_3 K_d - \beta_6 K_d'\right) \end{cases}$$

Assumption 2. The resultants of actuator faults related to modified quadrotor are bounded like follow:

$$|d_v| \le d_v^+, \quad v = \varphi, \theta, \psi, x, y, z \quad d_v^+ > 0 \quad (7)$$

3. Description of the interval type-2 fuzzy logic system

In this section, the interval type-2 fuzzy set and the inference of type-2 FLS are presented. The structure of an IT2FLS, as presented in Fig. 2, is quite similar to a T1FLS. The only difference is that the antecedent and/or consequent sets in an IT2FLS are type-2, so that each rule output set is a type-2. There are five principal parts in an IT2FLS: Fuzzifier, rule base, inference engine, type-reducer and defuzzifier.

The type-reducer performs a type-reduction operation which is an extended version of Type-1 defuzzification. Type reduction yields a Type-1 set from the Type-2 rule output set. The resulting T1 set is called type-reduced set. a crisp output could be obtained throughout defuzzifying the type-reduced set. The type reduced set of an IT2FIS shows the possible variation in the crisp output of the FLS due to the uncertain natures of the antecedents and/or consequents. The general form of the lth rule of the type-2 Takagi–Sugeno–Kang (TSK) fuzzy logic system can be written as:

$$If\, x_1 \text{ is } \widetilde{F}_1^l \text{ and } x_2 \text{ is } \widetilde{F}_2^l \text{ and } \ldots x_n \text{ is } \widetilde{F}_n^l, \text{ Than } y^l = \widetilde{G}^l l = \overline{1, M} \quad (8)$$

where:

The output of type-2 fuzzy system for the rule l is represented by $\widetilde{G}^l$, $x = [x_1, x_2, \ldots, x_n]^T$ are the inputs, the type-2 fuzzy system of the input state k of the lth rule is represented by $\widetilde{F}_k^l$, and M is the number of rules. As can be seen, the rule structure of type-2 fuzzy logic system is similar to type-1 fuzzy logic system except that type-1 membership functions are replaced with their type-2 counterparts. In Fig. 3, the footprint of uncertainty of

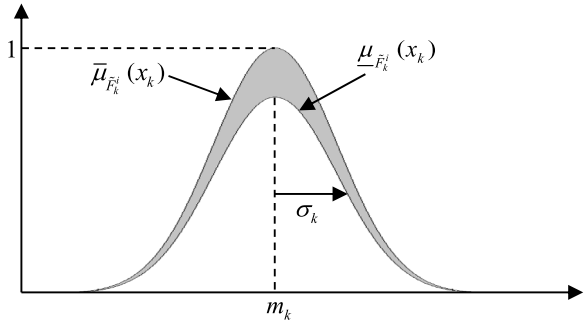

Fig. 3. Interval type-2 Gaussian MFs.

each membership function (MF) can be represented as a bounded interval in terms of the upper MF $\overline{\mu}_{\widetilde{F}_k^i}(x_k)$ and the lower $\underline{\mu}_{\widetilde{F}_k^i}(x_k)$, where

$$\overline{\mu}_{\widetilde{F}_k^i}(x_k) = \exp\left[-\frac{1}{2}\left(\frac{x_k - m_k}{\sigma_k}\right)\right] \text{ and } \underline{\mu}_{\widetilde{F}_k^i}(x_k) = 0.8\overline{\mu}_{\widetilde{F}_k^i}(x_k) \quad (9)$$

In fuzzy system interval type-2 using the minimum or product t-norms operations, the lth activated rule $F^i(x_1, \ldots, x_n)$ gives us the interval that is determined by two extremes $\underline{f}^l(x_1, \ldots, x_n)$ and $\overline{f}^l(x_1, \ldots, x_n)$ [53]:

$$F^l(x_1, \ldots, x_n) = \left[\underline{f}^l(x_1, \ldots, x_n), \overline{f}^l(x_1, \ldots, x_n)\right] \equiv \left[\underline{f}^l, \overline{f}^l\right] \quad (10)$$

With $\underline{f}^l$ and $\overline{f}^l$ are given as:

$$\begin{cases} \underline{f}^l = \underline{\mu}_{\widetilde{F}_1^i}(x_1) * \ldots * \underline{\mu}_{\widetilde{F}_n^i}(x_n) \\ \overline{f}^l = \overline{\mu}_{\widetilde{F}_1^i}(x_1) * \ldots * \overline{\mu}_{\widetilde{F}_n^i}(x_n) \end{cases} \quad (11)$$

There are many kinds of type-reduction, such as centroid, height, modified weight and center-of-sets [54,55]. The center-to-sets type-reduction will be used in this paper and can be expressed as:

$$Y = [y_L, y_R] = \int_{\theta^1} \cdots \int_{\theta^M} \cdots \int_{f^1} \cdots \int_{f^M} 1 \Big/ \frac{\sum_{i=1}^M f^l \theta^l}{\sum_{i=1}^M f^l} \quad (12)$$

Also, $\theta^l \in Y^l$ and $Y^l = \left[y_L^l, y_R^l\right]$ is the centroid of the type-2 interval consequent set $\widetilde{G}^l$, the centroid of a type-2 fuzzy set [56,57]. For any value $y \in Y$, y can be expressed as:

$$y = \frac{\sum_{i=1}^M f^l \theta^l}{\sum_{i=1}^M f^l} \quad (13)$$

where y is a monotonic increasing function with respect to θ^l. Also, y_L is the minimum associated only with y_L^l, and y_R is the

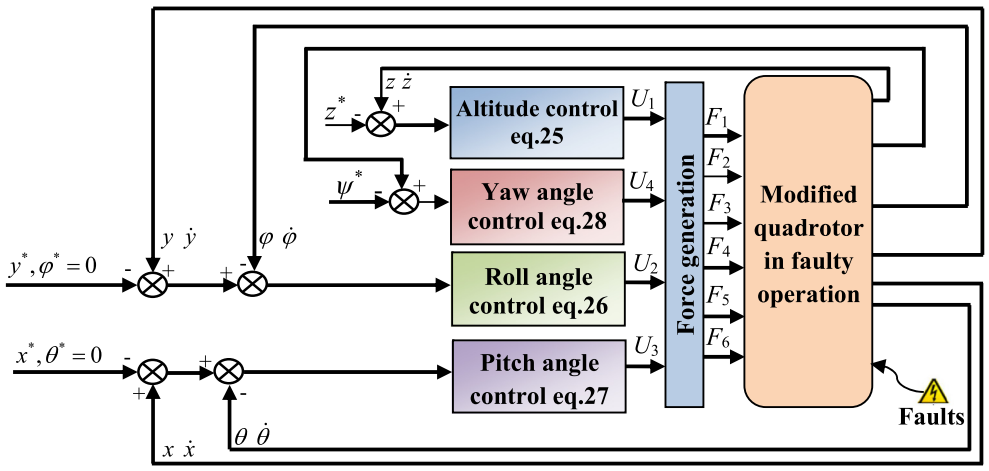

Fig. 4. Modified quadrotor control structure.

maximum associated only with y_R^l. Note that y_L and y_R depend only on the mixture off $\underline{f}^l$ or $\overline{f}^l$ values. Therefore, the left-most point y_L and the right-most point y_R can be expressed as a fuzzy basis function (FBF) expansion, i.e.,

$$y_L = \frac{\sum_{i=1}^{M} f_L^l \theta_L^l}{\sum_{i=1}^{M} f_L^l} = \sum_{i=1}^{M} \psi_L^l(x)\ \theta_L^l = \theta_L^T\ \psi_L^l(x) \tag{14}$$

where $\psi_L^l(x) = \frac{f_L^l}{\sum_{i=1}^{M} f_L^l}$ is the component of left FBF vectors that are defined by $\psi_L^T(x) = \left[\psi_L^1(x), \ldots, \psi_L^M(x)\right]$ and $\theta_L^T = \left[\theta_L^1, \ldots, \theta_L^M\right]$ is the left conclusion of IT2FLS.

$$y_R = \frac{\sum_{i=1}^{M} f_R^l \theta_R^l}{\sum_{i=1}^{M} f_R^l} = \sum_{i=1}^{M} \psi_R^l(x)\ \theta_R^l = \theta_R^T\ \psi_R^l(x) \tag{15}$$

where $\psi_R^l(x) = \frac{f_R^l}{\sum_{i=1}^{M} f_R^l}$ is the component of right FBF vectors that are defined by: $\psi_R^T(x) = \left[\psi_R^1(x), \ldots, \psi_R^M(x)\right]$ and $\theta_R^T = \left[\theta_R^1, \ldots, \theta_R^M\right]$ is the right conclusion of IT2FLS.

In order to compute Y, we need to compute y_L and y_R. This can be achieved by the use of the iterative Karnik Mendel algorithms procedure that is given in [53–55].

Initially we compute y_R

Without loss of generality, assume that θ_R^l are arranged in ascending order; i.e., $\theta_R^1 \le \theta_R^2 \le \cdots \le \theta_R^M$

1. Compute y_R in (15) by initially setting $f_R^l = \frac{\underline{f}^l + \overline{f}^l}{2}$ for $l = \overline{1, M}$ where $\underline{f}^l$ and $\overline{f}^l$ have been computed using (11), and let $y_R' = y_R$
2. Find k $(1 \le k \le M-1)$ such that $\theta_R^k \le y_R' \le \theta_R^{k+1}$.
3. Compute y_R in (15) with $f_R^l = \underline{f}^l$ for $l \le k$ and $f_R^l = \overline{f}^l$ for $l > k$; and let $y_R'' = y_R$
4. If $y_R'' \ne y_R'$, then go to step 5. If $y_R'' = y_R'$, then set $y_R = y_R''$ and go to step 6.
5. Set $y_R' = y_R''$, and return to step 2.
6. End

The procedure to compute y_L is similar to the one computing y_R in step 2, it only determines $k'\left(1 \le k' \le M-1\right)$, such that $\theta_L^{k'} \le y_L' \le \theta_L^{k'+1}$. In step 3, let $f_L^l = \overline{f}^l$ for $l \le k'$ and $f_L^l = \underline{f}^l$ for $l > k'$.

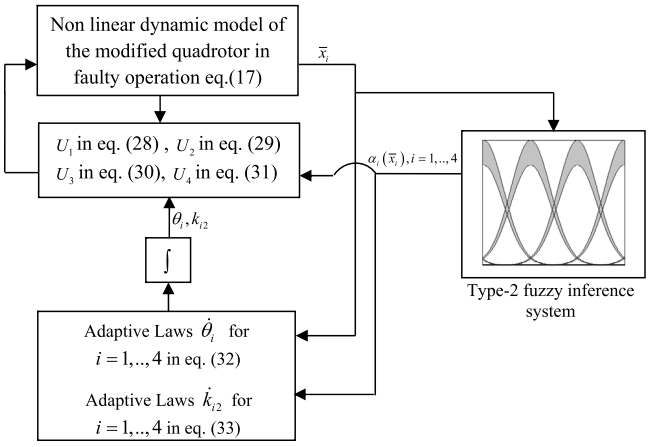

Fig. 5. Detailed block diagram of the proposed AT2FBC system.

The output of the type-2 fuzzy system is obtained by using the average value of y_R and y_L given by:

$$y = \frac{\theta_L^T \psi_L(x) + \theta_R^T \psi_R(x)}{2} = \theta^T\ \psi(x) \tag{16}$$

where $\psi^T(x) = \frac{1}{2}\left[\psi_L(x), \psi_R(x)\right]$ and $\theta^T = \left[\theta_L^T, \theta_R^T\right]$

4. Design of an adaptive type-2 fuzzy backstepping controller for modified quadrotor in presence actuators faults

The objective is to design an adaptive type-2 fuzzy backstepping control scheme for a modified quadrotor model in presence of actuators faults to handle correctly trajectory tracking. The role of the type-2 fuzzy systems is to approximate the local nonlinearities of each subsystem, while the fuzzy parameters are adjusted in real time by adaptive laws respecting the stability and convergence of the system according to the Lyapunov theory, in order to reach the desired tracking performance. To make easy the design of the proposed controller, we operate with the modified faulty quadrotor model developed in (5), in presence of

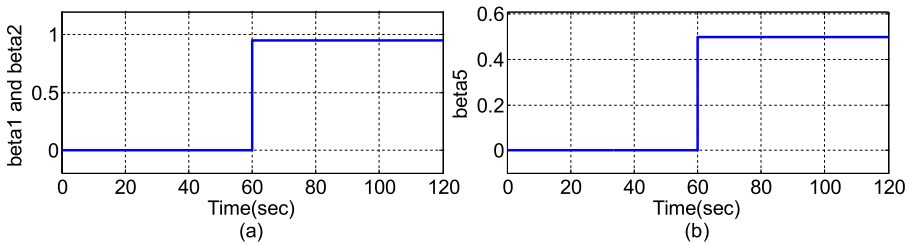

Fig. 6. Evaluation of the faults bias (β_1, β_2 and β_5).

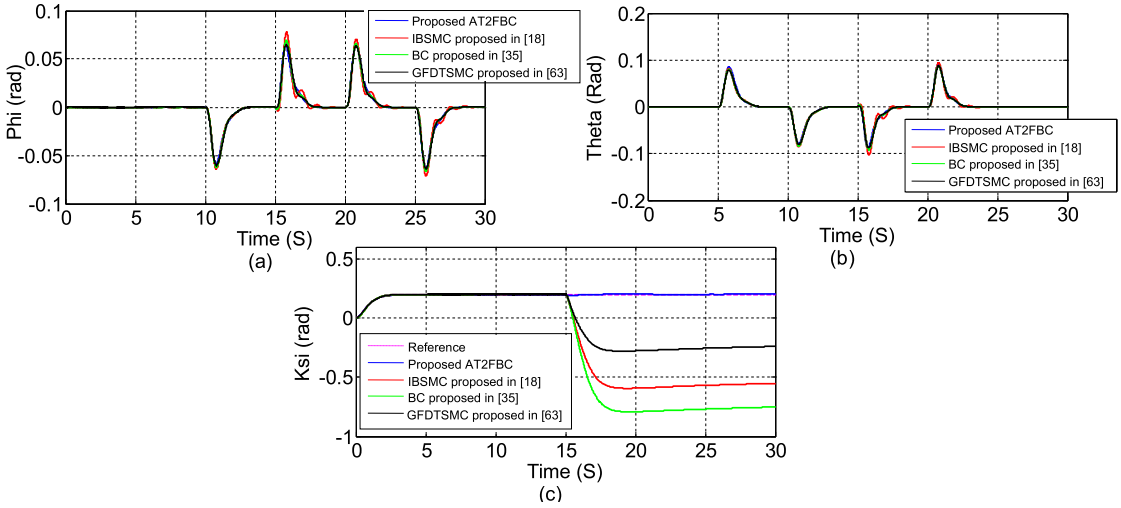

Fig. 7. Attitude subsystem tracking results of task 1: (a) tracking result of roll angle; (b) tracking result of pitch angle; (c) tracking result of yaw angle.

actuators faults:

$$\begin{cases} \ddot{z} = -\frac{1}{m}U_1(\cos\varphi\cos\theta) + g + f_1 \\ \ddot{\varphi} = \frac{1}{I_x}U_2 + f_2 \\ \ddot{\theta} = \frac{1}{I_y}U_3 + f_3 \\ \ddot{\psi} = \frac{1}{I_z}U_4 + f_4 \\ \ddot{x} = \frac{1}{m}U_1(\sin\theta) + f_5 \\ \ddot{y} = -\frac{1}{m}U_1(\sin\varphi\ \cos\theta) + f_6 \end{cases} \tag{17}$$

With $f_1, \ldots, f_6$ are unknown functions obtained by:

$$\begin{cases} f_1 = -\frac{k_3}{m}\dot{z} + d_z \\ f_2 = \frac{1}{I_x}\dot{\theta}\dot{\psi}\left(I_y - I_z\right) - \frac{k_4}{I_x}\dot{\varphi} - \frac{J_H\overline{\Omega}}{I_x}\dot{\theta} + d_\varphi \\ f_3 = \frac{1}{I_y}\dot{\varphi}\dot{\psi}\left(I_z - I_x\right) - \frac{k_5}{I_y}\dot{\theta} + \frac{J_H\overline{\Omega}}{I_y}\dot{\varphi} + d_\theta \\ f_4 = \frac{1}{I_z}\dot{\varphi}\dot{\theta}\left(I_x - I_y\right) - \frac{k_6}{I_z}\dot{\psi} + d_\psi \\ f_5 = -\frac{k_1}{m}\dot{x} + d_x \\ f_6 = -\frac{k_2}{m}\dot{y} + d_y \end{cases}$$

The type-2 fuzzy system is principally used to estimate any non-linearity $h_i(x_i)$ for $i = 1, \ldots, 4$. This estimation function, which can be approximated on compact set $\vartheta_{\bar{x}_i}$, is expressed as:

$$\hat{h}_i(\bar{x}_i) = \theta_i^T \alpha_i(\bar{x}_i), i = 1, \ldots, 4 \tag{18}$$

where: $\bar{x}_i$ is the input vector, θ_i is the adjusted vector parameters, and $\alpha_i(\bar{x}_i)$ is the average basis functions that are calculated using IT2FLS (each basis function is computed as the average of the corresponding left and right basis functions).

It can be define, the optimal value of θ_i as follows:

$$\theta_i^* = \underset{\theta_i}{Arg}\ \min\left[\sup_{x_i \in \vartheta_{\bar{x}_i}} \left|h_i(\bar{x}_i) - \hat{h}_i(\bar{x}_i)\right|\right] \tag{19}$$

In fact θ_i^*, used only for analysis purpose, is not needed during controller implementation [56–60].

The parameter estimation error is given by:

$$\tilde{\theta}_i = \theta_i^* - \theta_i \tag{20}$$

The type-2 fuzzy approximation error is defined by:

$$\overline{\omega}_i(\bar{x}_i) = h_i(\bar{x}_i) - \theta_i^{*T}\alpha_i(\bar{x}_i), i = 1, \ldots, 4 \tag{21}$$

As in the literature [56–60], the compact set $\vartheta_{\bar{x}_i}$ is assumed large enough so that the input vector of the type-2 fuzzy systems remains in $\vartheta_{\bar{x}_i}$ under the closed loop control system. Thus the type-2 fuzzy approximation error can be assumed to be bounded as follows:

$$|\overline{\omega}_i(\bar{x}_i)| \le \overline{\overline{\omega}}_i, \quad \forall \bar{x}_i \in \vartheta_{\bar{x}_i} \tag{22}$$

where $\overline{\overline{\omega}}_i$ are unknown positive parameters.

In order to achieve precise trajectory tracking, some assumptions have been adopted:

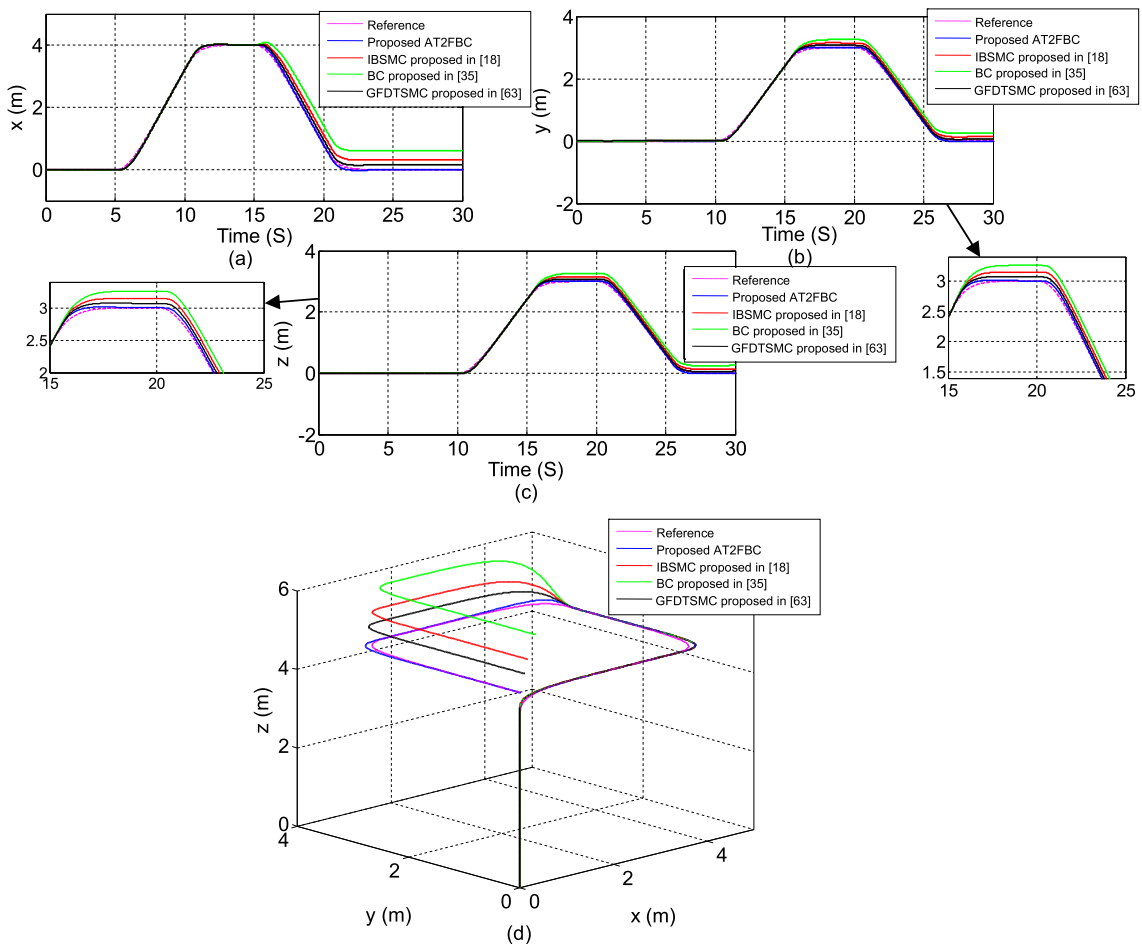

Fig. 8. Position subsystem tracking results of task 1: (a) tracking result of lateral position x; (b) tracking result of longitudinal position y; (c) tracking result of altitude position z; (d) 3D rectangle path tracking result.

Assumption 2. The reference signals $x^*, y^*, z^*, \varphi^*, \theta^*$ and ψ^* and their first derivatives are bounded and continuous.

Assumption 3. The three positions (x, y, z) and the three angles (φ, θ, ψ) are available for measurement.

The tracking errors and their filtered errors are given by:
For x position and θ angle [61]:

$$\widetilde{x}(t) = x(t) - x^*,\ \widetilde{\theta}(t) = \theta(t) - \theta^*,\ s_\theta = c_{1\theta}\dot{\widetilde{x}} + c_{2\theta}\widetilde{x} + \dot{\widetilde{\theta}} + c_{3\theta}\widetilde{\theta},\ \text{with } \widetilde{x}(0) = 0 \text{ and } \widetilde{\theta}(0) = 0 \quad (23)$$

For y position and φ angle [61]:

$$\widetilde{y}(t) = y(t) - y^*,\ \widetilde{\varphi}(t) = \varphi(t) - \varphi^*,$$
$$s_\varphi = c_{1\varphi}\dot{\widetilde{y}} + c_{2\varphi}\widetilde{y} + \dot{\widetilde{\varphi}} + c_{3\varphi}\widetilde{\varphi},\ \text{with } \widetilde{y}(0) = 0 \text{ and } \widetilde{\varphi}(0) = 0 \quad (24)$$

For z position:

$$\widetilde{z}(t) = z(t) - z^*,\ s_z = \dot{\widetilde{z}} + c_z\widetilde{z},\ \text{with } \widetilde{z}(0) = 0 \quad (25)$$

For ψ angle

$$\widetilde{\psi}(t) = \psi(t) - \psi^*,\ s_\psi = \dot{\widetilde{\psi}} + c_\psi\widetilde{\psi},\ \text{with } \widetilde{\psi}(0) = 0 \quad (26)$$

where $c_{1\theta}$, $c_{2\theta}$, $c_{3\theta}$, $c_{1\varphi}$, $c_{2\varphi}$, $c_{3\varphi}$, c_z and c_ψ are strictly positive design parameters, and we admit that:

$$\varphi^* = \theta^* = 0 \quad (27)$$

The following adaptive fuzzy control laws are made in the case where the dynamics of modified quadrotor is uncertain:

$$U_1 = \frac{-m}{cos\varphi\, cos\theta}\left(-\theta_1^T\alpha_1(\bar{x}_1) - g - k_{11}s_z - k_{12}\tanh\left(\frac{s_z}{\varepsilon_z}\right)\right) \quad (28)$$

$$U_2 = I_x\left(-\theta_2^T\alpha_2(\bar{x}_2) - k_{21}s_\varphi - k_{22}\tanh\left(\frac{s_\varphi}{\varepsilon_\varphi}\right)\right) \quad (29)$$

$$U_3 = I_y\left(-\theta_3^T\alpha_3(\bar{x}_3) - k_{31}s_\theta - k_{32}\tanh\left(\frac{s_\theta}{\varepsilon_\theta}\right)\right) \quad (30)$$

$$U_4 = I_z\left(-\theta_4^T\alpha_4(\bar{x}_4) - k_{41}s_\psi - k_{42}\tanh\left(\frac{s_\psi}{\varepsilon_\psi}\right)\right) \quad (31)$$

where: the design parameters k_{i2} remain constants for $i = 1, \ldots, 4$. $\varepsilon_z, \varepsilon_\varphi, \varepsilon_\theta$ and ε_ψ are absolutely positive design constants, usually of small values. tanh(.) is the abbreviation hyperbolic tangent function. The used interval type-2 fuzzy systems have as inputs, the following vectors: $\bar{x}_1 = [z, \dot{z}]^T$, $\bar{x}_2 = [\varphi, \dot{\varphi}]^T$, $\bar{x}_3 = \left[\theta, \dot{\theta}\right]^T$, $\bar{x}_4 = \left[\psi, \dot{\psi}\right]^T$. According to [56,62] and in order to estimate the unknown fuzzy vectors (θ_i^*) and the unknown parameters (k_{i2}^*) for $i = 1, \ldots, 4$, we adopt the following adaptive

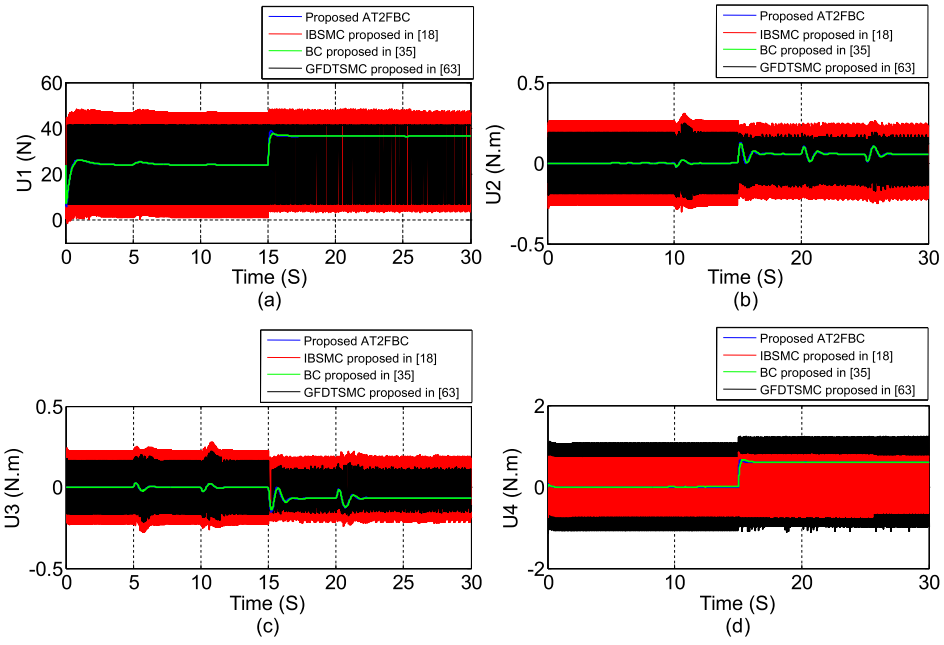

Fig. 9. Control force and torques results.

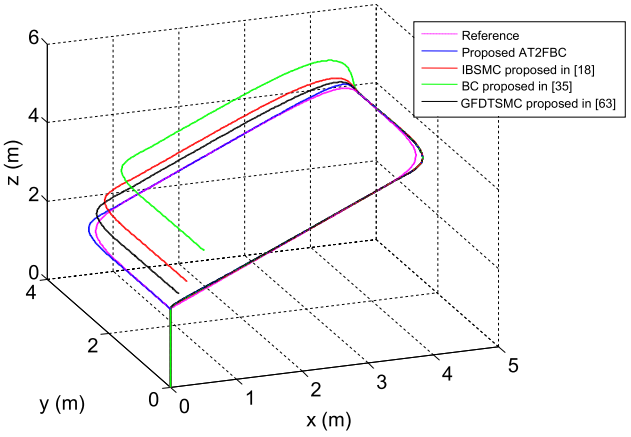

Fig. 10. Position tracking result of task 2.

laws:

$$\begin{cases} \dot{\theta}_1 = -\sigma_{\theta 1}\gamma_{\theta 1}\theta_1 + \gamma_{\theta 1}s_z\alpha_1\left(\bar{x}_1\right) \\ \dot{\theta}_2 = -\sigma_{\theta 2}\gamma_{\theta 2}\theta_2 + \gamma_{\theta 2}s_\varphi\alpha_2\left(\bar{x}_2\right) \\ \dot{\theta}_3 = -\sigma_{\theta 3}\gamma_{\theta 3}\theta_3 + \gamma_{\theta 3}s_\theta\alpha_3\left(\bar{x}_3\right) \\ \dot{\theta}_4 = -\sigma_{\theta 4}\gamma_{\theta 4}\theta_4 + \gamma_{\theta 4}s_\psi\alpha_4\left(\bar{x}_4\right) \end{cases} \tag{32}$$

$$\begin{cases} \dot{k}_{12} = -\sigma_{k1}\gamma_{k1}k_{12} + \gamma_{k1}s_z\tanh\left(\dfrac{s_z}{\varepsilon_z}\right) \\ \dot{k}_{22} = -\sigma_{k2}\gamma_{k2}k_{22} + \gamma_{k2}s_\varphi\tanh\left(\dfrac{s_\varphi}{\varepsilon_\varphi}\right) \\ \dot{k}_{32} = -\sigma_{k3}\gamma_{k3}k_{32} + \gamma_{k3}s_\theta\tanh\left(\dfrac{s_\theta}{\varepsilon_\theta}\right) \\ \dot{k}_{42} = -\sigma_{k4}\gamma_{k4}k_{42} + \gamma_{k4}s_\psi\tanh\left(\dfrac{s_\psi}{\varepsilon_\psi}\right) \end{cases} \tag{33}$$

where: $(\sigma_{\theta i}, \gamma_{\theta i}, \gamma_{ki}, \sigma_{ki}) > 0$ (for $i = 1, \ldots, 4$); these parameters are design constants.

Lemma 1. *The following properties are valid for a modified quadrotor modeled by Eq. (17) and controlled by the adaptive laws presented in Eqs. (32) and (33):*

- *The signals delimitation is guaranteed in closed-loop.*
- *The optimal choice of the setting parameters ensures the exponential convergence of the errors variables* $\widetilde{x}(t), \widetilde{y}(t), \widetilde{z}(t), \widetilde{\varphi}(t), \widetilde{\theta}(t)$ *and* $\widetilde{\psi}(t)$ *to insignificantly small residual set.*

The proof of Lemma 1 is based on Lyapunov's theory of stability. It is presented by a feedback structure with two consecutive steps.
Step 1: The purpose of this step is to lead the z position to its desired reference by an adequate speed controller.

Using the formula of the filtered z position error defined in (25):

$$s_z = \dot{\widetilde{z}} + c_z\widetilde{z}$$

From (17), the time derivative of s_z is:

$$\begin{aligned} \dot{s}_z &= -\frac{1}{m}U_1\left(\cos\varphi\cos\theta\right) + g + f_1 - \ddot{z}^* + c_z\left(\dot{z} - \dot{z}^*\right) \\ &= -\frac{1}{m}U_1\left(\cos\varphi\cos\theta\right) + g + h_1\left(\bar{x}_1\right) \end{aligned} \tag{34}$$

where: $h_1\left(\bar{x}_1\right) = f_1 - \ddot{z}^* + c_z\left(\dot{z} - \dot{z}^*\right)$

The Lyapunov function associated with the z position error is presented by:

$$V_1 = \frac{1}{2}s_z^2 \tag{35}$$

The time derivative of (35) is:

$$\dot{V}_1 = s_z\left(-\frac{1}{m}U_1\left(\cos\varphi\cos\theta\right) + g + h_1\left(\bar{x}_1\right)\right) \tag{36}$$

The following adaptive fuzzy system is developed to approximate the uncertain continuous function $h_1\left(\bar{x}_1\right)$

$$\begin{aligned} \hat{h}_1\left(\bar{x}_1\right) &= \theta_1^T\alpha_1\left(\bar{x}_1\right) \\ h_1\left(\bar{x}_1\right) &= \theta_1^{*T}\alpha_1\left(\bar{x}_1\right) + \varpi_1\left(\bar{x}_1\right) \\ &= -\widetilde{\theta}_1^T\alpha_1\left(\bar{x}_1\right) + \theta_1^T\alpha_1\left(\bar{x}_1\right) + \varpi_1\left(\bar{x}_1\right) \end{aligned} \tag{37}$$

where: $\widetilde{\theta}_1 = \theta_1 - \theta_1^*$ is the parameter error vector.

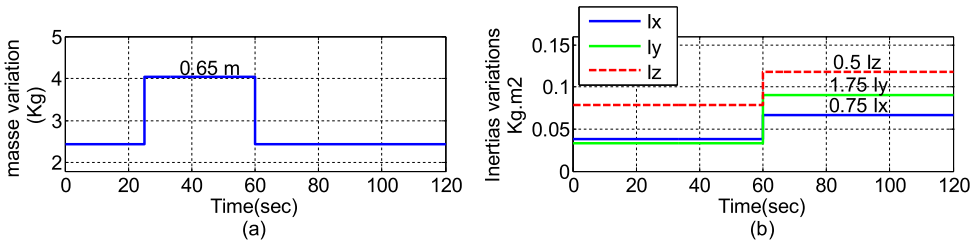

Fig. 11. Evolution of the parameters variations.

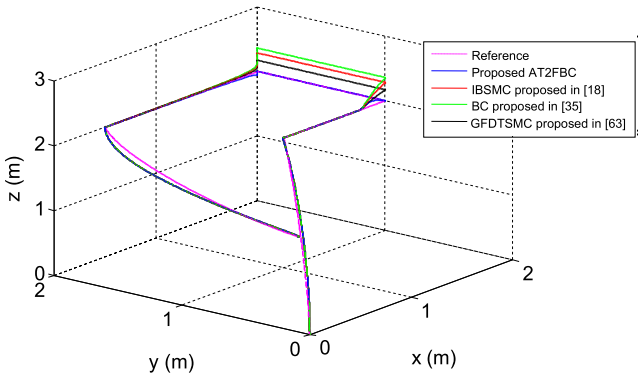

Fig. 12. Position tracking result of task 2.

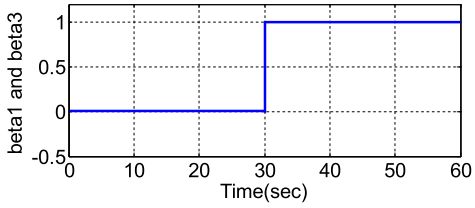

Fig. 13. Evaluation of the faults bias (β_1 and β_3)

By replacing (37) in (36), we obtain:

$$\dot{V}_1 = -s_z\widetilde{\theta}_1^T\alpha_1(\bar{x}_1) + s_z\theta_1^T\alpha_1(\bar{x}_1) + s_z\overline{\omega}_1(\bar{x}_1) + s_z g - s_z\frac{1}{m}U_1(\cos\varphi\cos\theta) \tag{38}$$

Where: $|\overline{\omega}_1(\bar{x}_1)| \le \overline{\overline{\omega}}_1, \quad \overline{\overline{\omega}}_1$: unknown constant (39)

By choosing the expression of U_1 presented in (28) and using (39), we can make the following inequality:

$$\dot{V}_1 \le -s_z\widetilde{\theta}_1^T\alpha_1(\bar{x}_1) + k_{12}^*|s_z| - k_{12}s_z\tanh\left(\frac{s_z}{\varepsilon_z}\right) - k_{11}s_z^2 \tag{40}$$

where: $k_{12}^* = \overline{\overline{\omega}}_1$.

Lemma 2. *the set* $\{\varepsilon_i > 0, x \in \Re\}$ *check the following inequality [56,62]:*

$$\begin{cases} 0 \le |x| - x\tanh\left(\dfrac{x}{\varepsilon_i}\right) \le \varepsilon_i = \rho\varepsilon_i \\ \rho = e^{-(1+\rho)} \simeq 0.2785 \end{cases} \tag{41}$$

By exploiting (41), (40) became:

$$\dot{V}_1 \le -s_z\widetilde{\theta}_1^T\alpha_1(\bar{x}_1) + k_{12}^*\bar{\varepsilon}_z - \widetilde{k}_{12}s_z\tanh\left(\frac{s_z}{\varepsilon_z}\right) - k_{11}s_z^2 \tag{42}$$

where $\widetilde{k}_{12} = k_{12} - k_{12}^*$ *and* $\bar{\varepsilon}_z = 0.2785\varepsilon_z$.

The Lyapunov function linked to the adaptive laws that estimate the unknown parameters θ_1^* *and* k_{12}^* *is defined by:*

$$V_2 = V_1 + \frac{1}{2\gamma_{\theta_1}}\widetilde{\theta}_1^T\widetilde{\theta}_1 + \frac{1}{2\gamma_{k_1}}\widetilde{k}_{12}^2 \tag{43}$$

The dynamics of Lyapunov function verify the following inequality:

$$\dot{V}_2 \le -s_z\widetilde{\theta}_1^T\alpha_1(\bar{x}_1) + k_{12}^*\bar{\varepsilon}_z - \widetilde{k}_{12}s_z\tanh\left(\frac{s_z}{\varepsilon_z}\right) - k_{11}s_z^2 + \frac{1}{2\gamma_{\theta_1}}\widetilde{\theta}_1^T\dot{\theta}_1 + \frac{1}{2\gamma_{k_1}}\widetilde{k}_{12}\dot{k}_{12} \tag{44}$$

By substituting the values of $\dot{\theta}_1$ *and* $\dot{k}_{12}$ *chosen in (32) and (33), respectively,* $\dot{V}_2$*will be bounded by the following expression:*

$$\dot{V}_2 \le k_{12}^*\bar{\varepsilon}_z - k_{11}s_z^2 - \sigma_{\theta_1}\widetilde{\theta}_1^T\theta_1 - \sigma_{k_1}\widetilde{k}_{12}k_{12} \tag{45}$$

Property.

$$\begin{cases} -\widetilde{\Theta}^T\Theta \le -\dfrac{1}{2}\left\|\widetilde{\Theta}\right\|^2 + \dfrac{1}{2}\left\|\Theta^*\right\|^2 \\ \widetilde{\Theta} = \Theta - \Theta^* \in \Re^m \end{cases} \tag{46}$$

where: m is a positive integer number.

Using (46), (45) takes the following form:

$$\dot{V}_2 \le -k_{11}s_z^2 - \frac{\sigma_{\theta_1}}{2}\left\|\widetilde{\theta}_1\right\|^2 - \frac{\sigma_{k_1}}{2}\widetilde{k}_{12}^2 + \bar{\varepsilon}_1 \tag{47}$$

With: $\bar{\varepsilon}_1 = k_{12}^*\bar{\varepsilon}_z + \frac{\sigma_{\theta_1}}{2}\left\|\theta_1^*\right\|^2 + \frac{\sigma_{k_1}}{2}k_{12}^{*2}$

The stabilization of the filtered errors s_φ, s_θ and $s_\psi$will be achieved in the following step.

Step 2: The aim of this step is to design the following control laws: U_2, U_3 and U_4.

The Lyapunov function adopted at this step is given by:

$$V_3 = V_2 + \frac{1}{2}s_\varphi^2 + \frac{1}{2}s_\theta^2 + \frac{1}{2}s_\psi^2 \tag{48}$$

The dynamics of Lyapunov function verify the following inequality:

$$\dot{V}_3 \le -k_{11}s_z^2 - \frac{\sigma_{\theta_1}}{2}\left\|\widetilde{\theta}_1\right\|^2 - \frac{\sigma_{k_1}}{2}\widetilde{k}_{12}^2 + \bar{\varepsilon}_1 + s_\varphi\dot{s}_\varphi + s_\theta\dot{s}_\theta + s_\psi\dot{s}_\psi \tag{49}$$

The derivatives of filtered errors s_φ, s_θ and s_ψ are obtained using Eq. (17):

$$\begin{cases} \dot{s}_\varphi = c_{1\varphi}\left(-\dfrac{1}{m}U_1(\sin\varphi\ \cos\theta) + f_6 - \ddot{y}^*\right) + c_{2\varphi}(\dot{y} - \dot{y}^*) \\ \qquad + \dfrac{1}{I_x}U_2 + f_2 - \dot{\varphi}^* + c_{3\varphi}(\dot{\varphi} - \dot{\varphi}^*) \\ \dot{s}_\theta = c_{1\theta}\left(\dfrac{1}{m}U_1(\sin\theta) + f_5 - \ddot{x}^*\right) + c_{2\theta}(\dot{x} - \dot{x}^*) \\ \qquad + \dfrac{1}{I_y}U_3 + f_3 - \dot{\theta}^* + c_{3\theta}(\dot{\theta} - \dot{\theta}^*) \\ \dot{s}_\psi = \dfrac{1}{I_z}U_4 + f_4 - \ddot{\psi}^* + c_\psi(\dot{\psi} - \dot{\psi}^*) \end{cases} \tag{50}$$

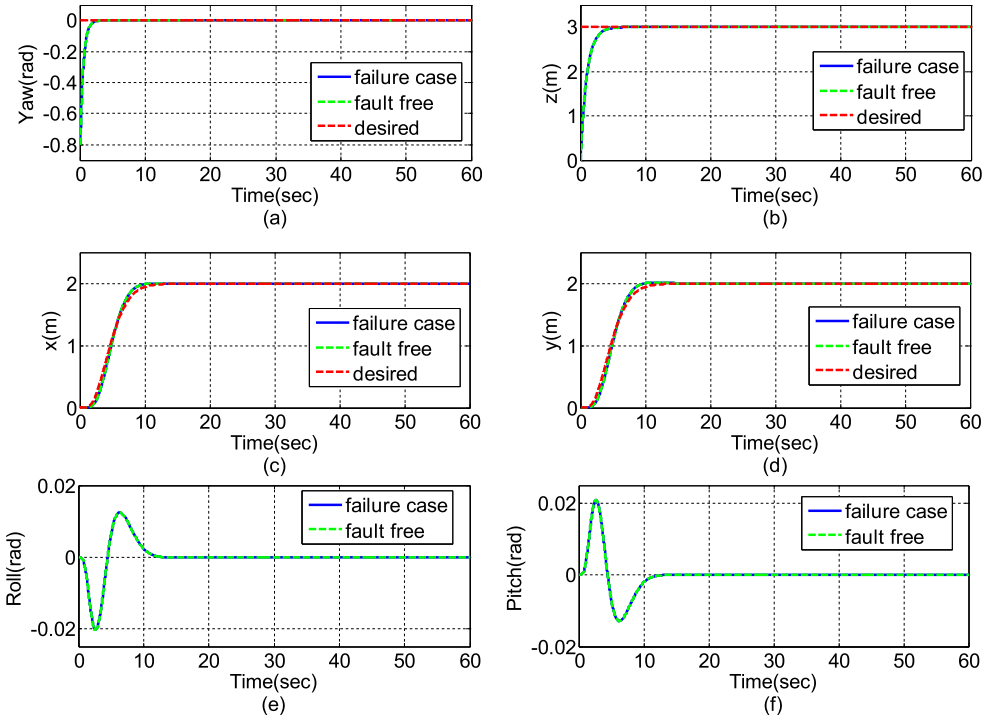

Fig. 14. Trajectory of the output variables in case rotor 1 and rotor 3 failure.

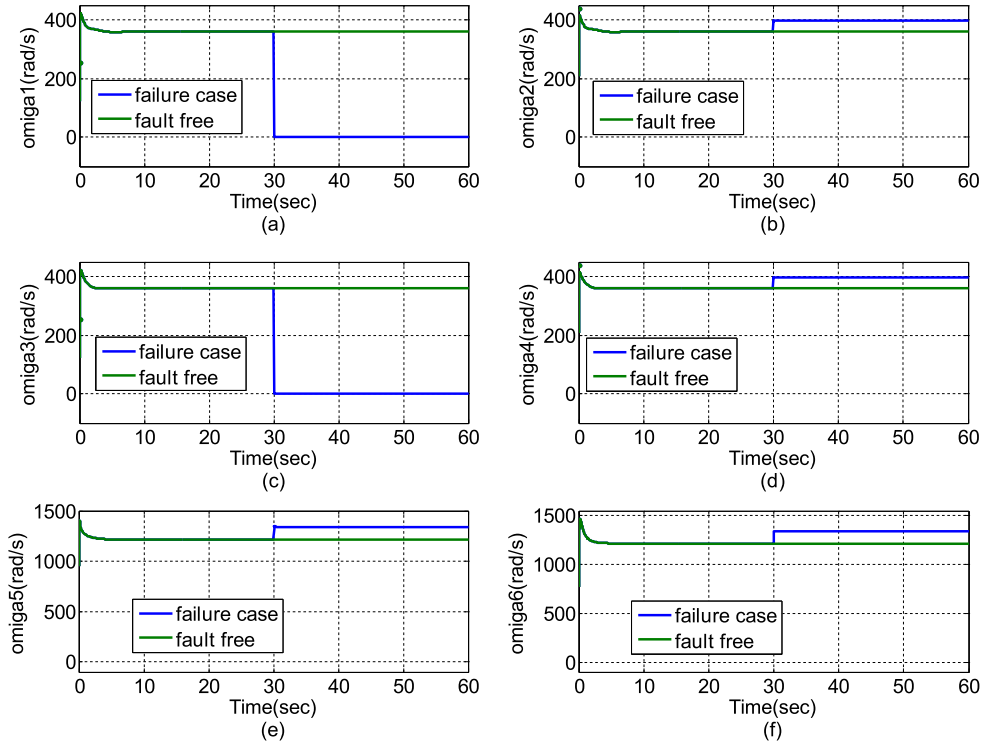

Fig. 15. Rotor speed in case rotor 1 and rotor 3 failure.

By replacing (50) in (49), we obtain:

$$\dot{V}_3 \leq -k_{11}s_z^2 - \frac{\sigma_{\theta_1}}{2}\left\|\widetilde{\theta}_1\right\|^2 - \frac{\sigma_{k_1}}{2}\widetilde{k}_{12}^2 + \bar{\varepsilon}_1 + s_\varphi\left(h_2(\bar{x}_2) + \frac{1}{I_x}U_2\right) + s_\theta\left(h_3(\bar{x}_3) + \frac{1}{I_y}U_3\right) + s_\psi\left(h_4(\bar{x}_4) + \frac{1}{I_z}U_4\right) \quad (51)$$

where:

$$\begin{cases} h_2(\bar{x}_2) = c_{1\varphi}\left(-\frac{1}{m}U_1(\sin\varphi\ \cos\theta) + f_6 - \ddot{y}^*\right) \\ \qquad + c_{2\varphi}(\dot{y} - \dot{y}^*) + f_2 - \dot{\varphi}^* + c_{3\varphi}(\dot{\varphi} - \dot{\varphi}^*) \\ h_3(\bar{x}_3) = c_{1\theta}\left(\frac{1}{m}U_1(\sin\theta) + f_5 - \ddot{x}^*\right) + c_{2\theta}(\dot{x} - \dot{x}^*) \\ \qquad + f_3 - \dot{\theta}^* + c_{3\theta}(\dot{\theta} - \dot{\theta}^*) \\ h_4(\bar{x}_4) = f_4 - \ddot{\psi}^* + c_\psi(\dot{\psi} - \dot{\psi}^*) \end{cases}$$

$h_i(\bar{x}_i)$, $i = 2, 3, 4$ are continuous uncertainties functions, their approximation is performed by the following adaptive fuzzy system:

$$\begin{aligned} \hat{h}_i(\bar{x}_i) &= \theta_i^T\alpha_i(\bar{x}_i) \\ h_i(\bar{x}_i) &= \theta_i^{*T}\alpha_i(\bar{x}_i) + \bar{\omega}_i(\bar{x}_i) \\ &= -\widetilde{\theta}_i^T\alpha_i(\bar{x}_i) + \theta_i^T\alpha_i(\bar{x}_i) + \bar{\omega}_i(\bar{x}_i) \ \text{ for } i = 2, 3, 4 \end{aligned} \quad (52)$$

where: $\widetilde{\theta} = \theta_i - \theta_i^*$ expresses the error vector, $\bar{x}_i$ is pre-defined, $\bar{\omega}_i(\bar{x}_i)$ is the fuzzy approximation error with $|\bar{\omega}_i(\bar{x}_i)| \leq \bar{\bar{\omega}}_i, \forall\, \bar{x}_i \in D_{\bar{x}i}$, $\bar{\bar{\omega}}_i$ is an unknown constant.

If we select the adaptive fuzzy controller components proposed in (29)–(31) and the continuous uncertainties functions $h_i(\bar{x}_i)$ developed in (52), $\dot{V}_3$ will be bounded by the following term:

$$\begin{aligned} \dot{V}_3 \leq{}& -k_{11}s_z^2 - \frac{\sigma_{\theta_1}}{2}\left\|\widetilde{\theta}_1\right\|^2 - \frac{\sigma_{k_1}}{2}\widetilde{k}_{12}^2 + \bar{\varepsilon}_1 - s_\varphi\widetilde{\theta}_2^T\alpha_2(\bar{x}_2) \\ &+ k_{22}^*|s_\varphi| - k_{22}s_\varphi\tanh\left(\frac{s_\varphi}{\varepsilon_\varphi}\right) - k_{21}s_\varphi^2 - s_\theta\widetilde{\theta}_3^T\alpha_3(\bar{x}_3) + \\ &k_{32}^*|s_\theta| - k_{32}s_\theta\tanh\left(\frac{s_\theta}{\varepsilon_\theta}\right) - k_{31}s_\theta^2 - s_\psi\widetilde{\theta}_4^T\alpha_4(\bar{x}_4) \\ &+ k_{42}^*|s_\psi| - k_{42}s_\psi\tanh\left(\frac{s_\psi}{\varepsilon_\psi}\right) - k_{41}s_\psi^2 \end{aligned} \quad (53)$$

where $k_{22}^* = \bar{\bar{\omega}}_2$, $k_{32}^* = \bar{\bar{\omega}}_3$, and $k_{42}^* = \bar{\bar{\omega}}_4$.

By exploiting (41), the inequality (53) becomes:

$$\begin{aligned} \dot{V}_3 \leq{}& -k_{11}s_z^2 - \frac{\sigma_{\theta_1}}{2}\left\|\widetilde{\theta}_1\right\|^2 - \frac{\sigma_{k_1}}{2}\widetilde{k}_{12}^2 + \bar{\varepsilon}_1 - s_\varphi\widetilde{\theta}_2^T\alpha_2(\bar{x}_2) \\ &+ k_{22}^*\bar{\varepsilon}_\varphi - \widetilde{k}_{22}s_\varphi\tanh\left(\frac{s_\varphi}{\varepsilon_\varphi}\right) - k_{21}s_\varphi^2 - s_\theta\widetilde{\theta}_3^T\alpha_3(\bar{x}_3) + \\ &k_{32}^*\bar{\varepsilon}_\theta - \widetilde{k}_{32}s_\theta\tanh\left(\frac{s_\theta}{\varepsilon_\theta}\right) - k_{31}s_\theta^2 - s_\psi\widetilde{\theta}_4^T\alpha_4(\bar{x}_4) \\ &+ k_{42}^*\bar{\varepsilon}_\psi - \widetilde{k}_{42}s_\psi\tanh\left(\frac{s_\psi}{\varepsilon_\psi}\right) - k_{41}s_\psi^2 \end{aligned} \quad (54)$$

where: $\widetilde{k}_{22} = k_{22} - k_{22}^*$, $\widetilde{k}_{32} = k_{32} - k_{32}^*$, $\widetilde{k}_{42} = k_{42} - k_{42}^*$, $\bar{\varepsilon}_\varphi = 0.2785\,\varepsilon_\varphi$, $\bar{\varepsilon}_\theta = 0.2785\,\varepsilon_\theta$ and $\bar{\varepsilon}_\psi = 0.2785\,\varepsilon_\psi$ $\left\{\theta_i^*, k_{i2}^*\right\}$ $i = 2, 3, 4$ are unknown parameters, their estimation requires an adaptive law defined by the following Lyapunov function:

$$V_4 = V_3 + \frac{1}{2\gamma_{\theta_2}}\widetilde{\theta}_2^T\widetilde{\theta}_2 + \frac{1}{2\gamma_{k_2}}\widetilde{k}_{22}^2 + \frac{1}{2\gamma_{\theta_3}}\widetilde{\theta}_3^T\widetilde{\theta}_3 + \frac{1}{2\gamma_{k_3}}\widetilde{k}_{32}^2 + \frac{1}{2\gamma_{\theta_4}}\widetilde{\theta}_4^T\widetilde{\theta}_4 + \frac{1}{2\gamma_{k_4}}\widetilde{k}_{42}^2 \quad (55)$$

The derivation of (55) gives:

$$\begin{aligned} \dot{V}_4 \leq{}& -k_{11}s_z^2 - \frac{\sigma_{\theta_1}}{2}\left\|\widetilde{\theta}_1\right\|^2 - \frac{\sigma_{k_1}}{2}\widetilde{k}_{12}^2 + \bar{\varepsilon}_1 - s_\varphi\widetilde{\theta}_2^T\alpha_2(\bar{x}_2) \\ &+ k_{22}^*\bar{\varepsilon}_\varphi - \widetilde{k}_{22}s_\varphi\tanh\left(\frac{s_\varphi}{\varepsilon_\varphi}\right) - k_{21}s_\varphi^2 - s_\theta\widetilde{\theta}_3^T\alpha_3(\bar{x}_3) + \\ &k_{32}^*\bar{\varepsilon}_\theta - \widetilde{k}_{32}s_\theta\tanh\left(\frac{s_\theta}{\varepsilon_\theta}\right) - k_{31}s_\theta^2 - s_\psi\widetilde{\theta}_4^T\alpha_4(\bar{x}_4) + k_{42}^*\bar{\varepsilon}_\psi \\ &- \widetilde{k}_{42}s_\psi\tanh\left(\frac{s_\psi}{\varepsilon_\psi}\right) - k_{41}s_\psi^2 + \frac{1}{2\gamma_{\theta_2}}\widetilde{\theta}_2^T\dot{\theta}_2 + \frac{1}{2\gamma_{k_2}}\widetilde{k}_{22}\dot{k}_{22} + \\ &\frac{1}{2\gamma_{\theta_3}}\widetilde{\theta}_3^T\dot{\theta}_3 + \frac{1}{2\gamma_{k_3}}\widetilde{k}_{32}\dot{k}_{32} + \frac{1}{2\gamma_{\theta_4}}\widetilde{\theta}_4^T\dot{\theta}_4 + \frac{1}{2\gamma_{k_4}}\widetilde{k}_{42}\dot{k}_{42} \end{aligned} \quad (56)$$

By using (46), we obtain:

$$\begin{aligned} \dot{V}_4 \leq{}& -k_{11}s_z^2 - \frac{\sigma_{\theta_1}}{2}\left\|\widetilde{\theta}_1\right\|^2 - \frac{\sigma_{k_1}}{2}\widetilde{k}_{12}^2 - k_{21}s_\varphi^2 - \frac{\sigma_{\theta_2}}{2}\left\|\widetilde{\theta}_2\right\|^2 \\ &- \frac{\sigma_{k_2}}{2}\widetilde{k}_{22}^2 - k_{31}s_\theta^2 - \frac{\sigma_{\theta_3}}{2}\left\|\widetilde{\theta}_3\right\|^2 - \frac{\sigma_{k_3}}{2}\widetilde{k}_{32}^2 - k_{41}s_\psi^2 - \\ &\frac{\sigma_{\theta_4}}{2}\left\|\widetilde{\theta}_4\right\|^2 - \frac{\sigma_{k_4}}{2}\widetilde{k}_{42}^2 + \bar{\varepsilon}_1 + \bar{\varepsilon}_2 + \bar{\varepsilon}_3 + \bar{\varepsilon}_4 \end{aligned} \quad (57)$$

where:

$$\begin{aligned} \bar{\varepsilon}_2 &= k_{22}^*\bar{\varepsilon}_\varphi + \frac{\sigma_{\theta_2}}{2}\left\|\theta_2^*\right\|^2 + \frac{\sigma_{k_2}}{2}k_{22}^{*2}, \\ \bar{\varepsilon}_3 &= k_{32}^*\bar{\varepsilon}_\varphi + \frac{\sigma_{\theta_3}}{2}\left\|\theta_3^*\right\|^2 + \frac{\sigma_{k_3}}{2}k_{32}^{*2}, \\ \bar{\varepsilon}_4 &= k_{42}^*\bar{\varepsilon}_z + \frac{\sigma_{\theta_4}}{2}\left\|\theta_4^*\right\|^2 + \frac{\sigma_{k_4}}{2}k_{42}^{*2} \end{aligned}$$

A simplified form of (54) can be presented as follow:

$$\dot{V}_4 \leq -\eta\, V_4 + \mu \quad (58)$$

With:

$$\mu = \bar{\varepsilon}_1 + \bar{\varepsilon}_2 + \bar{\varepsilon}_3 + \bar{\varepsilon}_4, \quad \eta_k = \min\left\{\sigma_{k_1}\gamma_{k_1}, \sigma_{k_2}\gamma_{k_2}, \sigma_{k_3}\gamma_{k_3}, \sigma_{k_4}\gamma_{k_4}\right\}$$

And

$$\eta = \min\left\{2k_{11}, 2k_{21}, 2k_{31}, 2k_{41}, \sigma_{\theta_1}\gamma_{\theta_1}, \sigma_{\theta_2}\gamma_{\theta_2}, \sigma_{\theta_3}\gamma_{\theta_3}, \sigma_{\theta_4}\gamma_{\theta_4}, \eta_k\right\}$$

If we multiply (58) by the exponential term $e^{\eta t}$, we obtain [56,63]:

$$\frac{d}{dt}\left(V_4 e^{\eta t}\right) \leq \mu e^{\eta t} \quad (59)$$

The integration of (57) from 0 to t yields:

$$0 \leq V_4 \leq \frac{\mu}{\eta} + \left(V_4(0) - \frac{\mu}{\eta}\right)e^{-\eta t} \quad (60)$$

where: μ is a randomly selected parameter and η is chosen according to the design parameters. According to [56,62], the bounded interval of V_4 presented by (57) reflects the exponential convergence to an adaptable residual set for tracking errors, filtered tracking errors and parameter estimation errors, besides the delimitation of all closed-loop signals. The global block diagram of the proposed FTC is shown in Fig. 4.

The detailed block diagram of the proposed AT2FBC system is presented in Fig. 5.

5. Simulation results

To investigate the efficiency and the performance attained for the trajectory tracking problem, we simulate the proposed control strategy. The parameters of modified quadrotor system are given as [1]: $m = 2.45$ kg, $l = 0.25$ m, the nominal values of I_x, I_y and I_z are $(I_x, I_y, I_z) = diag(3.8\times10^{-2}, 3.3\times10^{-2}, 7.9\times10^{-2})$ kg m^2, $K_t = 7\times10^{-7}$ N s^2, $K_t' = 8\times10^{-6}$ N s^2, $K_d = 1\times10^{-8}$ N m s^2, $K_d' = 4\times10^{-7}$ N m s^2, $J_H = 5\times10^{-4}$ kg m^2, $k_1 =$

Table 1
Control parameters of proposed AT2FBC.

Variable	Value
k_{j1}, $j = 1, \ldots, 4$	2
k_{j2}, $j = 1, \ldots, 4$	1
$\sigma_{\theta 1}$, $j = 1, \ldots, 4$	10^{-2}
$\gamma_{\theta j}$, $j = 1, \ldots, 4$	100
σ_{kj}, $j = 1, \ldots, 4$	10^{-1}
ε_v, $v = z, \varphi, \theta, \psi$	10^{-3}

Table 2
Control parameters of compared controllers.

Controllers	Design simulation parameters
Zhenyue et al. Controller [19]	$K = \begin{bmatrix} K_1 & 0 \\ 0 & K_2 \end{bmatrix}$, $K_1 = 3I_{3\times3}$, $K_2 = 0.9\,I_{3\times3}$ $A = \begin{bmatrix} A_1 & 0 \\ 0 & A_2 \end{bmatrix}$, $A_1 = 1.5I_{6\times6}$, $K_2 = 9\,I_{6\times6}$ $\varepsilon_1 = 10$, $\varepsilon_2 = 2$ $Q = \begin{bmatrix} Q_1 & 0 \\ 0 & Q_2 \end{bmatrix}$, $Q_1 = 5I_{3\times3}$, $Q_2 = 50\,I_{3\times3}$
Mohamad Ali et al. Controller [1]	$\alpha_1 = \alpha_3 = \alpha_5 = 2.8$, $\alpha_2 = \alpha_4 = \alpha_6 = 3.75$, $\lambda_1 = \lambda_3 = \lambda_5 = 15.94$, $\lambda_2 = \lambda_4 = \lambda_6 = 52.42$
Jing-Jing et al. Controller [64]	$c_z = c_\psi = \beta_1 = \beta_2 = m_1 = m_2 = c_3 = c_7 = 1$ $\eta_3 = \eta_4 = \beta_3 = \beta_4 = m_3 = m_4 = 1$, $\varepsilon_1 = \varepsilon_2 = 30$, $\eta_1 = \eta_2 = 2$, $\alpha_1 = \alpha_2 = \varepsilon_3 = \varepsilon_4 = \alpha_3 = \alpha_4 = 10$, $m_1^{'} = m_2^{'} = m_3^{'} = m_4^{'} = 7$, $n_1^{'} = n_2^{'} = n_3^{'} = n_4^{'} = 9$, $n_1 = n_2 = n_3 = n_4 = 3$, $c_4 = c_8 = 6$, $c_1 = 12m/(u_1 \cos\varphi \cos\psi)$, $c_2 = 8m/(u_1 \cos\varphi \cos\psi)$, $c_5 = -12m/(u_1 \cos\psi)$ $c_6 = -8m/(u_1 \cos\psi)$

$k_2 = k_3 = 10^{-3}$ N/m/s, $k_4 = k_5 = k_6 = 1.2\times10^{-3}$ N/rad/s. The faults is assumed to occur at $t = 60$ s with 95% loss of control effectiveness in the first and second motor ($\beta_1 = \beta_2 = 0.95$), and 50% loss in the fifth motor ($\beta_5 = 0.5$). The evaluation of the faults bias (β_1, β_2 and β_5) are given in Fig. 6. The vectors $\bar{x}_1 = [z, \dot{z}]^T$, $\bar{x}_2 = [\varphi, \dot{\varphi}]^T$, $\bar{x}_3 = \left[\theta, \dot{\theta}\right]^T$, $\bar{x}_4 = \left[\psi, \dot{\psi}\right]^T$ represent the inputs of the type-2 fuzzy systems $\theta_i^T \alpha_i(\bar{x}_i)$ for $i = 1, \ldots, 4$. For the variables $\left(z, \dot{z}, \varphi, \dot{\varphi}, \theta, \dot{\theta}, \psi, \dot{\psi}\right)$, we define five type-2 Gaussian membership functions uniformly distributed on the intervals $[-1, 1]$. Note that all the design adaptive parameters in those control systems are chosen to achieve a satisfactory transient control performance considering the requirement of stability and all variable states of the modified quadrotor are considered measurable and available to the controllers. For the proposed AT2FBC system, one has chosen the design parameters summarized in Table 1.

In order to verify the effectiveness and robustness of the proposed AT2FBC strategy, simulations for four typical flight tasks in faulty operation mode are carried out on Matlab/ Simulink environment. Besides, backstepping control (BC) proposed in [1], global fast dynamic terminal sliding mode control (GFDTSMC) proposed in [64] and integral backstepping sliding mode control (IBSMC) proposed in [19] are introduced as comparison counterparts to demonstrate the superiority of the proposed control method. The parameters required for implementing these three controllers are listed in Table 2.

Task 1.

Track a horizontal rectangle as follows, and fix the desired yaw angle at 0.2 rad with initial conditions chosen as $(x_0, y_0, z_0, \psi_0) = (0, 0, 0, 0)$ [65].

$$\begin{cases} x_d = \dfrac{4(t-5)}{5} fsg(t, 5, 10) + 4\, fsg(t, 10, 15) \\ \qquad + \dfrac{4(20-t)}{5} fsg(t, 15, 20) \\ y_d = \dfrac{3(t-10)}{5} fsg(t, 10, 15) + 3\, fsg(t, 15, 20) \\ \qquad + \dfrac{3(25-t)}{5} fsg(t, 20, 25) \\ x_d = \dfrac{3t}{5} fsg(t, 0, 5) + 3\, fsg(t, 5, 30) \end{cases}$$

$$fsg(x, a, b) = \frac{sign(x-a) + sign(b-x)}{2}$$

The contrast simulation results of the proposed method BC, GFDTSMC, and IBSMC are depicted in Figs. 7 and 8.

Fig. 7 shows the attitude tracking simulation results of the three methods. It is obvious that the proposed strategy has the best tracking performance. This is quite remarkable when observing the tracking result of yaw angle, where the BC, GFDTSMC and IBSMC, failed to make the attitude angles track their references. This is due to the fact that these control techniques are sensitive to the mismatched disturbances (the actuator faults). The results confirm that the proposed control strategy has better robustness and control performances even in the presence of actuator faults.

According to simulation results of faulty operation mode presented in Fig. 8; before the fault occurrence, the desired trajectories are successfully tracked for both control strategies (BC, GFDTSMC, IBSMC and the proposed AT2FBC). But, after the occurrence of actuators faults, (after $t = 15$ s), the actual trajectories according to (x, y and z) positions (Fig. 8 (a–d)) corresponding to the BC, GFDTSMC and IBSMC are deviated from their desired trajectories. The reason for the poor tracking performance of BC, GFDTSMC and IBSMC is that the inner attitude loop has no ability to counteract the actuator fault impacts without adaptation of the controller. In fact, since, the multi-rotor aircraft is an underactuated system, translational motion is realized through attitude motion. Good control performance of the inner attitude subsystem is a basis for the outer loop trajectory tracking control. Therefore, the inaccurate control for attitude system further causes the failure of outer loop to track the desired trajectory under various adverse factors. This proves the need of an adaptive attitude control to ensure a good trajectory tracking under actuator fault, which is adopted by using type-2 fuzzy inference system.

From the simulation results presented in Fig. 9, it is clearly observable that the control result of the GFDTSMC and IBSMC produces a significant chattering phenomenon. On the contrary, the chattering phenomenon of the controlled system was suppressed in the BC and proposed AT2FBSMC.

For GFDTSMC and IBSMC, the conventional switching action in the control law still causes severe chattering issue. Evidently, the proposed AT2FBSMC strategy successfully eliminates the chattering in the control action, which makes it more suitable for the actual applications. Furthermore, control actions showed a sufficiently enough variations to compensate the impact of actuator faults (Fig. 9). This former is estimated by using an adaptive type-2 fuzzy inference system.

Task 2.

Track a slant rectangle in space expressed as follows, and fix the desired yaw angle at 0.2 rad with initial conditions chosen as $(x_0, y_0, z_0, \psi_0) = (0, 0, 0, 0)$ [65].

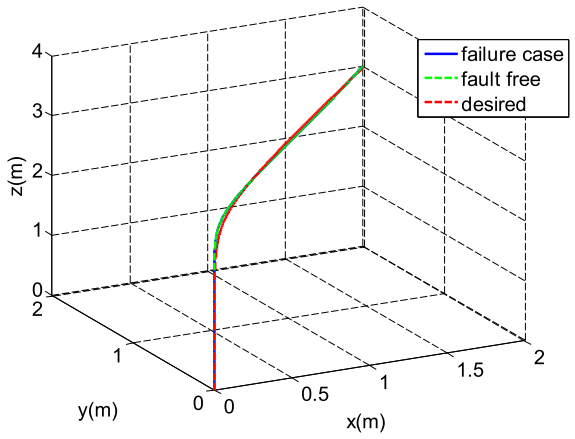

Fig. 16. Absolute position of the modified quadrotor in case rotor (1, 3) failure.

$$\begin{cases} x_d = \dfrac{4(t-5)}{5} fsg(t,5,10) + 4\, fsg(t,10,15) \\ \qquad + \dfrac{4(20-t)}{5} fsg(t,15,20) \\ y_d = \dfrac{3(t-10)}{5} fsg(t,10,15) + 3\, fsg(t,15,20) \\ \qquad + \dfrac{3(25-t)}{5} fsg(t,20,25) \\ x_d = 2 + \dfrac{3(t-5)}{5} fsg(t,0,5) + 3\, fsg(t,10,15) \\ \qquad + \dfrac{3(20-t)}{5} fsg(t,15,20) \end{cases}$$

where

$$fsg(x,a,b) = \frac{sign(x-a) + sign(b-x)}{2}$$

Fig. 10 shows the slant rectangle trajectory tracking results of the proposed control strategy, BC, GFDTSMC and IBSMC. The aircraft can still track the slant rectangle perfectly using the proposed method with a better performance over the other three methods.

Task 3. Flight with uncertainties of the inertias and the masse

BC, GFDTSMC and IBSMC and the proposed AT2FBC are simulated under inertias and masse uncertainties like presented in Fig. 11 with initial conditions chosen as $(x_0, y_0, z_0, \psi_0) = (0, 0, 0, 0)$. In this simulation, the control objective is to evaluate the altitude trajectory tracking performances with inertias and masse variations (Fig. 12).

Fig. 12 shows the position tracking simulation results. Similarly, the modified quadrotor aircraft is able to track the desired reference trajectories in nominal conditions when using BC, GFDTSMC and IBSMC as shown in Fig. 12. However, the degenerate performance response shown in altitude curvature presented in the same figure is resulted mainly under masse variation. On the contrary, the proposed control strategy accomplished the tracking task excellently in both of nominal and masse variation modes.

The simulation results of all flight tasks validate the effectiveness and the strong robustness of the proposed control strategy against actuator faults as well as masse variation.

Task 4. Flight with rotor 1 and rotor 3 failure

Figs. 13–16 shows simulation results when rotor 1, and rotor 3 fail at 30 s ($\beta_1 = \beta_3 = 1$) with initial conditions chosen as $(x_0, y_0, z_0, \psi_0) = (0, 0, 0, -0.8)$. Fig. 14(a–f) shows no visible degradation in performance when compared to the fault free case which highlights the efficacy of the proposed AT2FBC. On the other hand, Fig. 15(a) and (c) clearly shows the speed of rotor 1 and rotor 3 dropping to zero at 30 s The control signal is redistributed to rotors 2, 4, 5 and 6 showing an increase in these rotors speeds in order to compensate the failed ones. Fig. 16, presenting the absolute 3D-position of the modified quadrotor during its flight, with ($\beta_1 = \beta_3 = 1$), shows that the assigned navigational task is successfully achieved and the reference trajectory is tracked with high accuracy.

Table 3
IAE performance indexes.

State	Proposed AT2FBC	GFDTSMC proposed in [64]	IBSMC proposed in [19]	BC proposed in [1]
x	1.4676	4.65	5.813	7.267
y	1.6185	3.720	5.152	6.441
z	0.1092	7.376	9.220	11.525
φ	0.1936	0.125	0.157	0.197
θ	0.1974	0.130	0.16	0.20
ψ	0.0259	10.03	12.512	15.640

A quantitative comparison in faulty operating mode (Task 1) is also made between the four previous control methods based on integral absolute error (IAE) criterion. The results are listed in Table 3.

In case of faulty operating mode of the modified quadrotor aircraft, it is noted that the proposed AT2FBC offers the smallest values of IAE, whereas the control methods proposed in [1,19,64] present the largest ones for almost all states. It can be concluded that the system performances are better, when using the proposed AT2FBC as compared to the control methods proposed in [1,19,64].

6. Conclusion

In this paper, the adaptive controller based on backstepping and type-2 fuzzy systems has been investigated, in the presence of external disturbances, parametric variations and actuator faults. This control law incorporates adaptive parameters to compensate the external disturbances effect, actuator faults and the reconstruction errors. The application of the developed method is carried out for a modified quadrotor aircraft proposed in [1]. The obtained simulation results show that the developed AT2FBC maintains the tracking errors in an acceptable interval, even in the presence of actuator faults, significant parameter variations or external disturbances. The simple nature of the proposed approach makes it easily implementable in real-time control systems.

In addition, the comparative study between the proposed control approach and other works developed in the literature has shown the effectiveness and robustness of the proposed control approach. As a future work, a complete onboard implementation of the presented approach will be realized on a low-cost embedded processor. Moreover, the width of the type-2 membership functions will be tuned in an adaptive manner in order to obtain better performance.

Declaration of competing interest

The authors declare that they have no known competing financial interests or personal relationships that could have appeared to influence the work reported in this paper.

References

[1] Mohamad AT, Mohamad JM, Moosa A. Dynamic modeling and nonlinear tracking control of a novel modified quadrotor. Internat J Robust Nonlinear Control 2018;28(2):552–67.
[2] Qingsong J, Jia L, Yunxi Z. Analysis and design the controller for quadrotors based on PID control method. In: Proceedings of the IEEE international conference on chinese association of automation. 2018, p. 88–92.
[3] Abdel-Razzak M, Hassan N, François B. Emergency control of AR drone quadrotor UAV suffering a total loss of one rotor. IEEE/ASME Trans Mechatronics 2017;22(2):961–71.
[4] Yihao W, Chuanjiang L, Yanchao S. Backstepping approach for controlling a quadrotor using Barrier Lyapunov Functions. In: Proceedings of the IEEE international conference on chinese control conference. 2017, p. 6235–9.
[5] Ali S, Muhammad NM. Lyapunov-based nonlinear controller for quadrotor position and attitude tracking with GA optimization. In: Proceedings of the IEEE international conference on industrial electronics and applications conference. 2016, p. 342–7.
[6] Zhiwei X, Xiaohong N, Haibo W, Chen Yinsheng. Robust guaranteed cost tracking control of quadrotor UAV with uncertainties. ISA Trans 2017;(69):157–65.
[7] Gianluca A, Elisabetta C, Filippo A, Paolo RG, Stefano C, Antonio F. Adaptive trajectory tracking for quadrotor MAVs in presence of parameter uncertainties and external disturbances. IEEE Trans Control Syst Technol 2018;26(1):248–54.
[8] Yao Z, Bing Z. Adaptive trajectory tracking controller for quadrotor systems subject to parametric uncertainties. J Franklin Inst B 2017;345(15):6724–46.
[9] Anjali BS, Vivek A, Nandagopal JL. Simulation and analysis of integral LQR controller for inner control loop design of a fixed wing micro aerial vehicle (MAV). Procedia Technol 2016;25:76–83.
[10] Ramin A, Rasul F, Mohammad AK. Updating LQR control for full dynamic of a quadrotor. In: Proceedings of the IEEE international conference on robotics and mechatronics. 2017, p. 279–85.
[11] Changlong L, Jian P, Chang Yufang. PID And LQR trajectory tracking control for an unmanned quadrotor helicopter: Experimental studies. In: Proceedings of the IEEE international conference on chinese control conference. 2016, p. 10845–50.
[12] Juan PO, Luis IM, Manuel JR. Nonlinear robust H-infinity PID controller for the multivariable system quadrotor. IEEE Lat Am Trans 2016;14(3):1176–83.
[13] Bailing T, Yuxin M, Zong Qun. A continuous finite-time output feedback control scheme and its application in quadrotor UAVs. IEEE Access 2018;6:19807–13.
[14] Dong EC, Yongsoon E. Global chartwise feedback linearization of the quadcopter with a thrust positivity preserving dynamic extension. IEEE Trans Automat Control 2017;62(9):4747–52.
[15] Rui W, Jinkun L. Trajectory tracking control of a 6-DOF quadrotor UAV with input saturation via backstepping. J Franklin Inst B 2018;355(7):3288–309.
[16] Hao L, Cunjia L, Matthew C, Lei G, Wen-Hua C. Online optimisation-based backstepping control design with application to quadrotor. IET Control Theory Appl 2016;10(14):1601–11.
[17] Juntao F, Cheng L. Adaptive sliding mode control of dynamic systems using double loop recurrent neural network structure. IEEE Trans Neural Netw Learn Syst 2018;29(4):1275–86.
[18] Manuel JR, Luis IM, Ortiz Paul, Darwin FA, Diego V. Paul ortiz darwin f.a diego v trajectory tracking of a quadrotor using sliding mode control. IEEE Lat Am Trans 2016;14(5):2157–66.
[19] Zhenyue J, Jianqiao Y, Yuesong M, Yongbo C, Yuanchuan S, Xiaolin A. Integral backstepping sliding mode control for quadrotor helicopter under external uncertain disturbances. Aerosp Sci Technol 2017;68:299–307.
[20] Filiberto M, Iván G, Sergio S, Eduardo SE, Rogelio L. Second order sliding mode controllers for altitude control of a quadrotor UAS: Real-time implementation in outdoor environments. Neurocomputing 2017;233:61–71.
[21] Iman S, Abbas C, Youmin Z, Didier T. Control allocation and re-allocation for a modified quadrotor helicopter against actuator faults. In: Proceedings of the 8th IFAC symposium on fault detection, supervision and safety of technical processes. 2012, p. 247–52.
[22] Juan G, Claudio D, Alejandro G, Ignacio M. Experimental validation of a fault-tolerant hexacopter with tilted rotors. Int J Electr Electron Eng Telecommun 2018;7:58–65.
[23] Halim A, Christopher E. Sliding mode fault-tolerant control of an octorotor using linear parameter varying-based schemes. IET Control Theory Appl 2015;9:618–36.
[24] Guang-Xun D, Quan Q, Kai-Yuan C. Controllability analysis and degraded control for a class of hexacopters subject to rotor failures. J Intell Robot Syst 2015;78:143–57.
[25] Juan G, Ricardo S, Alejandro S. Analysis and design of a tilted rotor hexacopter for fault tolerance. IEEE Trans Aerosp Electron Syst 2016;52:1555–67.
[26] Ban W, Youmin Z. An adaptive fault-tolerant sliding mode control allocation scheme for multirotor helicopter subject to simultaneous actuator faults. IEEE Trans Ind Electron 2018;65:4227–36.
[27] Guillermo F, Valentin M, Florian H. Fault tolerant control for a hexarotor system using incremental backstepping. In: Proceedings of the IEEE control applications. 2016, p. 237–42.
[28] Halim A, Mirza H, Christopher E. An integral sliding mode fault tolerant control scheme for an octorotor using fixed control allocation. In: Proceedings of the IEEE workshop on variable structure systems. 2014, p. 1–6.
[29] Majd S, Benjamin L, Isabelle F, Hassan S, Clovis F. Fault diagnosis and fault-tolerant control of an octorotor UAV using motors speeds measurements. In: Proceedings of the 20th IFAC world congress. 2017, p. 5263–8.
[30] Halim A, Christopher E. Fault tolerant control of octorotor using sliding mode control allocation. In: Proceedings of the 2nd CEAS specialist conference on guidance, navigation & control. 2013, p. 1404–23.
[31] Samir Z, Djamel S, Kamel. Fault tolerant control based on neural network interval type-2 fuzzy sliding mode controller for octorotor UAV. Front Comput Sci 2016;10:657–72.
[32] Abdel-Razzak M, François B, Hassan N. Passive and active fault tolerant control of octorotor UAV using second order sliding mode control. In: Proceedings of the IEEE conference on control applications. 2015, p. 1907–12.
[33] Majd S, Hassan S, Clovis F, Isabelle F, Benjamin L. Actuator fault diagnosis in an octorotor UAV using sliding modes technique: Theory and experimentation. In: Proceedings of the european control conference. 2015, p. 1639–44.
[34] Majd S, Benjamin L, Isabelle F, Hassan S, Clovis F. Passive fault-tolerant control of an octorotor using super-twisting algorithm: Theory and experiments. In: Proceedings of the 3rd conference on control and fault-tolerant systems. 2016, p. 361–6.
[35] Samir Z, Hemza M, Abderrahmen B, Ali D. Actuator fault tolerant control using adaptive RBFNN fuzzy sliding mode controller for coaxial octorotor UAV. ISA Trans 2018;80:267–78.
[36] Dezhi X, Xiaojie S, Peng S. Adaptive command-filtered fuzzy backstepping control for linear induction motor with unknown end effect. Inform Sci 2019;477:118–31.
[37] Yongming L, Shaocheng T, Tieshan L. Hybrid fuzzy adaptive output feedback control design for uncertain MIMO nonlinear systems with time-varying delays and input saturation. IEEE Trans Fuzzy Syst 2016;24:841–53.
[38] Bouguerra A, Saigaa D, Kara K, Zeghlache S. Fault-tolerant lyapunov-gain-scheduled PID control of a quadrotor UAV. Int J Intell Eng Syst 2015;8(2):1–6.
[39] Xu D, Ferris J, Cooke WA. Fault tolerant control of a quadrotor using L1 adaptive control. Int J Intell Unmanned Syst 2016;4(1):1–20.
[40] Erdal K, Reinaldo M. Type-2 fuzzy logic trajectory tracking control of quadrotor VTOL aircraft with elliptic membership functions. IEEE/ASME Trans Mechatronics 2017;22(1):339–48.
[41] Chen F, Jiang R, Zhang K, Jiang B. Robust backstepping sliding mode control and observer-based fault estimation for a quadrotor UAV. IEEE Trans Ind Electron 2016;63(8):5044–56.
[42] Chen F, Lei W, Tao G, Jiang B. Actuator fault estimation and reconfiguration control for the quad-rotor helicopter. Int J Adv Robot Syst 2017;13(1):1–12.
[43] Feng-ying Z, Hua-jun G, Zi-yang Z. Adaptive constraint backstepping fault-tolerant control for small carrier-based unmanned aerial vehicle with uncertain parameters. Proc Inst Mech Eng G 2016;230(3):1–19.
[44] Taleb A, Sepideh S, Cai-Hua X, Jiang-Feng Y. Simplified fuzzy-Padé controller for attitude control of quadrotor helicopters. IET Control Theory Appl 2018;12(2):310–7.
[45] Changhong F, Andriy S, Erdal K, Christian W, Robert J, Jonathan MG. Input uncertainty sensitivity enhanced nonsingleton fuzzy logic controllers for long-term navigation of quadrotor UAVs. IEEE/ASME Trans Mechatronics 2018;23(2):725–34.
[46] Andrew Z, Samuel J. A review of control algorithms for autonomous quadrotors. Open J Appl Sci 2014;4:547–56.
[47] Kuantama E, Vesselenyi T, Dzitac S, Tarca R. PID and Fuzzy-PID control model for quadcopter attitude with disturbance parameter. Int J Comput Commun Control 2017;12(4):519–32.
[48] Gianluca A, Elisabetta C, Filippo A, Paolo RG, Stefano C, Antonio F. Adaptive trajectory tracking for quadrotor MAVs in presence of parameter uncertainties and external disturbances. IEEE Trans Control Syst Technol 2018;26(1):248–54.
[49] Dailiang M, Yuanqing X, Ganghui S, Zhiqiang J, Tianya L. Flatness-based adaptive sliding mode tracking control for a quadrotor with disturbances. J Franklin Inst B 2018;355(14):6300–22.
[50] Tung TP, Dang HL, Chi-Ngon N, Tu DN, Cuong CT. Optimizing the structure of RBF neural network-based controller for omnidirectional mobile robot control. In: Proceedings of the international conference on system science and engineering. 2017, p. 313–8.

[51] Saeed B, Mohammad AB, Mohammad RJ. Improved adaptive fuzzy sliding mode controller for robust fault tolerant of a quadrotor. Int J Control Autom Syst 2017;15(1):427–41.
[52] Abdel-Razzak M, Hassan N, François B. Active fault tolerant control of quadrotor UAV using sliding mode control. In: Proceedings of the international conference on unmanned aircraft systems. 2014, p. 156–66.
[53] Yifan L, Zhiqiang P, Jianqiang Y. Observer-based robust adaptive Type-2 fuzzy tracking control for flexible air-breathing hypersonic vehicles. IET Control Theory Appl 2018;12(8):1036–45.
[54] Andriy S, Changhong F, Erdal K, Tufan K. Type-2 fuzzy logic controllers made even simpler: From design to deployment for UAVs. IEEE Trans Ind Electron 2018;65(6):5069–77.
[55] El-Nagar Ahmad M. Nonlinear dynamic systems identification using recurrent interval type-2 TSK fuzzy neural network – A novel structure. ISA Trans 2018;72:205–17.
[56] Bounar N, Boulkroune A, Boudjema F, M'Saad M, Farza M. Adaptive fuzzy vector control for a doubly-fed induction motor. Neurocomputing 2015;151(Pt 2):756–69.
[57] Boulkroune A, M'saad M. A fuzzy adaptive variable-structure control scheme for uncertain chaotic MIMO systems with sector nonlinearities and dead zones. Expert Syst Appl 2011;38:14744–50.
[58] Boulkroune A, M'saad M. On the design of observer-based fuzzy adaptive controller for nonlinear systems with unknown control gain sign. Fuzzy Sets System 2012;201:71–85.
[59] Wang WY, Leu YG, Lee TT. Output-feedback control of nonlinear systems using direct adaptive fuzzy-neural controller. Fuzzy Sets System 2003;140:341–58.
[60] Tong S, Li HX, Chen GR. Adaptive fuzzy decentralized control for a class of large-scale nonlinear systems. IEEE Trans Syst Man Cybern B 2004;134:770–5.
[61] En-Hui Z, Jing-Jing X, Ji-Liang L. Second order sliding mode control for a Quadrotor UAV. ISA Trans 2014;53(4):1350–6.
[62] Yacef F, Bouhali O, Hamerlain M, Rizoug N. Observer-based adaptive fuzzy backstepping tracking control of quadrotor unmanned aerial vehicle powered by Li-ion battery. J Intell Robot Syst 2016;84:179–97.
[63] Jinzhu P, Rickey D. Adaptive fuzzy backstepping control for a class of uncertain nonlinear strict-feedback systems based on dynamic surface control approach. Expert Syst Appl 2019;120:239–52.
[64] Jing-Jing X, Guo-Bao Z. Global fast dynamic terminal sliding mode control for a quadrotor UAV. ISA Trans 2017;66(4):233–40.
[65] Chunyang F, Yantao T, Cheng P, Xun G, Lei Z, Xiaojun G. Sensor faults tolerance control for a novel multi-rotor aircraft based on sliding mode control. Proc Inst Mech Eng G 2017. http://dx.doi.org/10.1177/0954410017731590.